Searching New Materials for Energy Conversion and Energy Storage

R. NESPER ETH ZÜRICH & COLLEGIUM HELVETICUM

1. Renewable Energy
2. Solar Cells
3. Thermoelectricity
4. Fast High Energy Li-Ion Batteries
5. Light Emitting Devices
6. Hydrogen Storage
7. Luminescent Materials
8. New Materials

Renewable Energies

R. NESPER ETH ZÜRICH & COLLEGIUM HELVETICUM

1. **Solar energy**
2. **Geo thermal**
3. **Water power**
4. **Wind power**
5. **Bio energy**

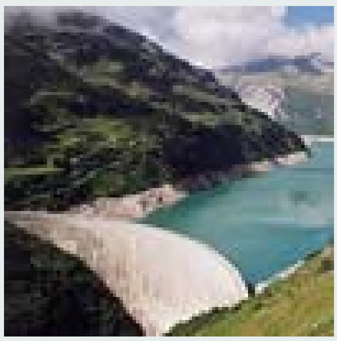

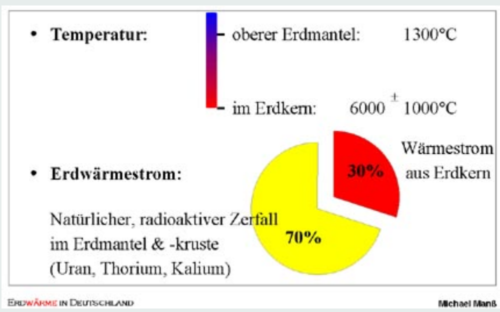

Renewable Energy Management

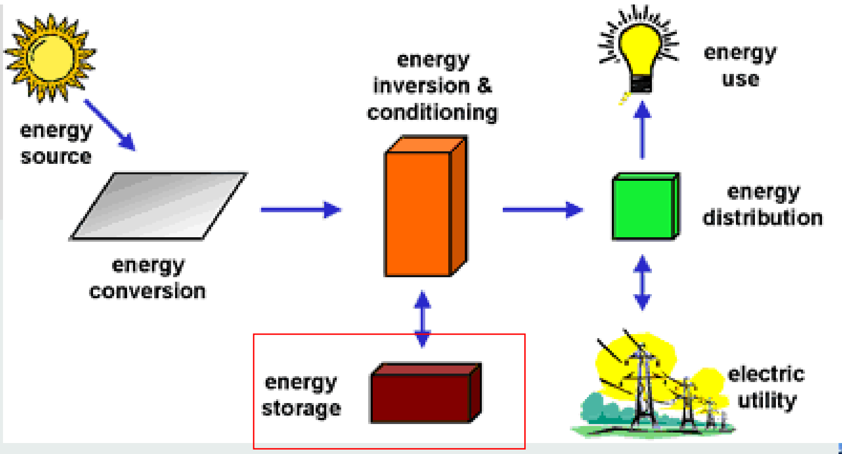

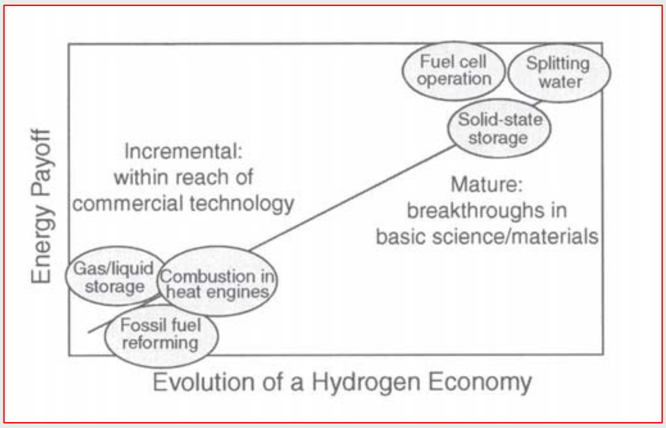

R. NESPER ETH ZÜRICH & COLLEGIUM HELVETICUM

Geo Thermal Energy

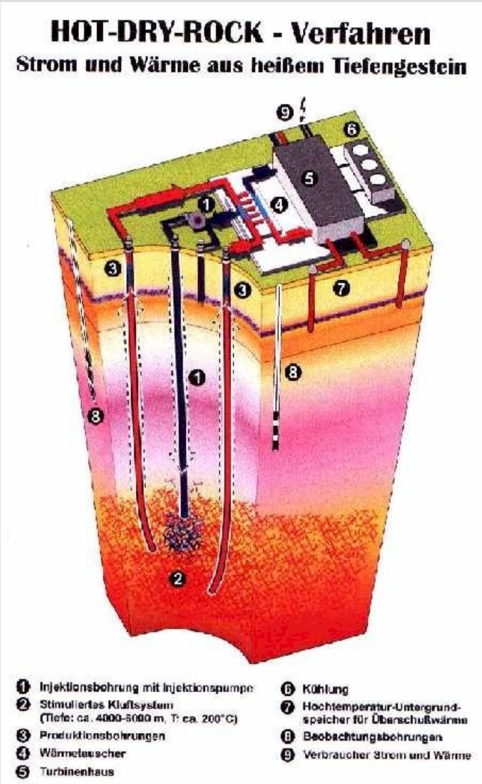

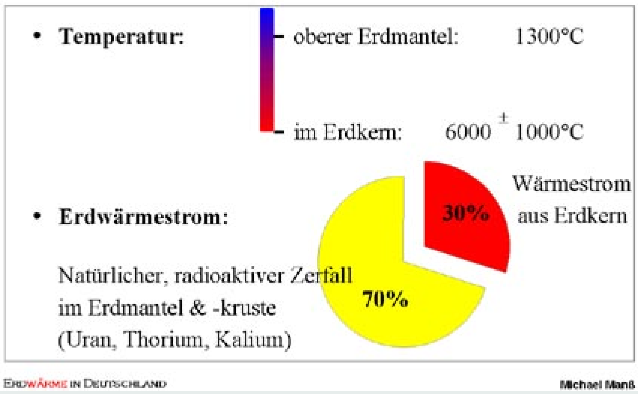

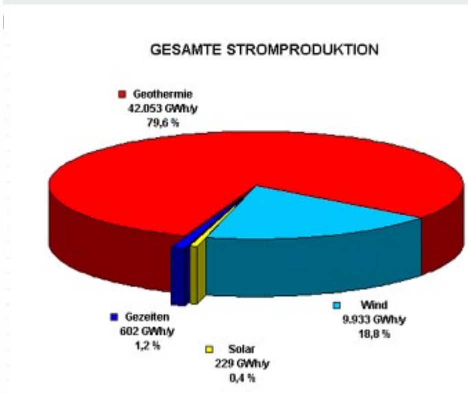

R. NESPER ETH ZÜRICH & COLLEGIUM HELVETICUM

Solar Energy

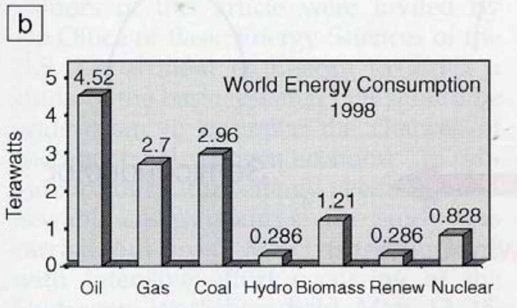

"At some point, almost certainly within this decade, we will peak in the amount of oil that is produced worldwide."

"To give all 10 billion people on the planet the level of energy prosperity we in the developed world are used to, a couple of kilowatt-hours per person, we would need to generate 60 terawatts around the planet—the equivalent of 900 million barrels of oil per day."

Figure 3. Solar cell land area requirements in which the six boxes (100 km on a side), located in areas of high solar radiation, can each provide 3.3 terawatts of electrical power to a total of ~20 terawatts of electrical power. Courtesy of Nate Lewis of the California Institute of Technology.

Searching New Materials for Energy Conversion and Energy Storage

1. Renewable Energy
2. **Solar Cells**
3. Thermoelectricity
4. Fast High Energy Li-Ion Batteries
5. Light Emitting Devices
6. Hydrogen Storage
7. Luminescent Materials
8. New Materials

Solar Energy Spectrum

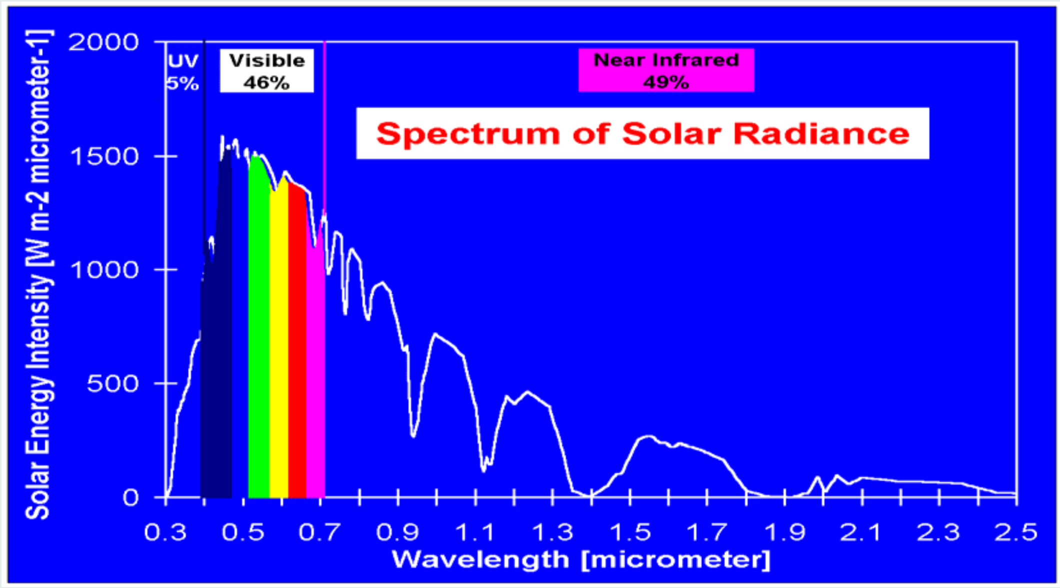

- **Power reaching earth 1.37 kW/m²**

Solar Cells - Better than Biology ?

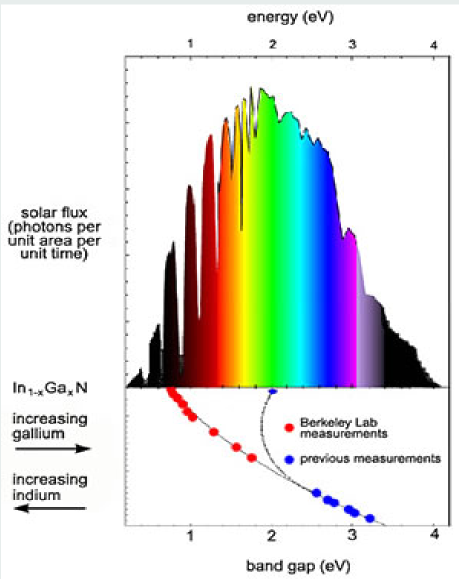

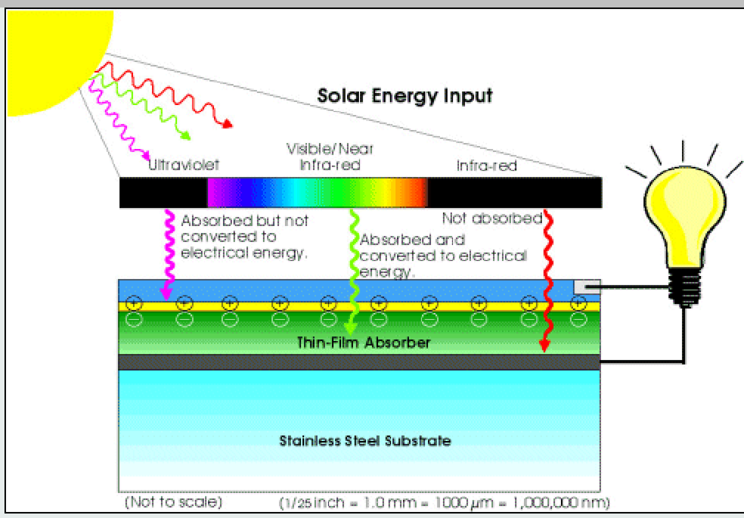

A newly established low band gap for indium nitride means that the indium gallium nitride system of alloys ($In_{1-x}Ga_xN$) covers the full solar spectrum

Solar cell – Working Principle

- Operating diode in fourth quadrant generates power

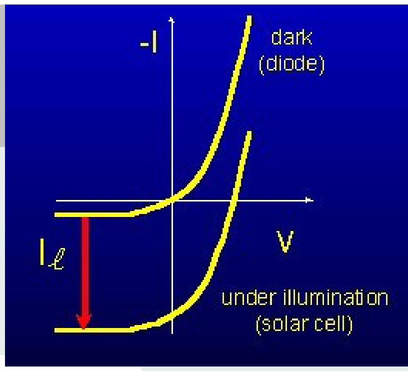

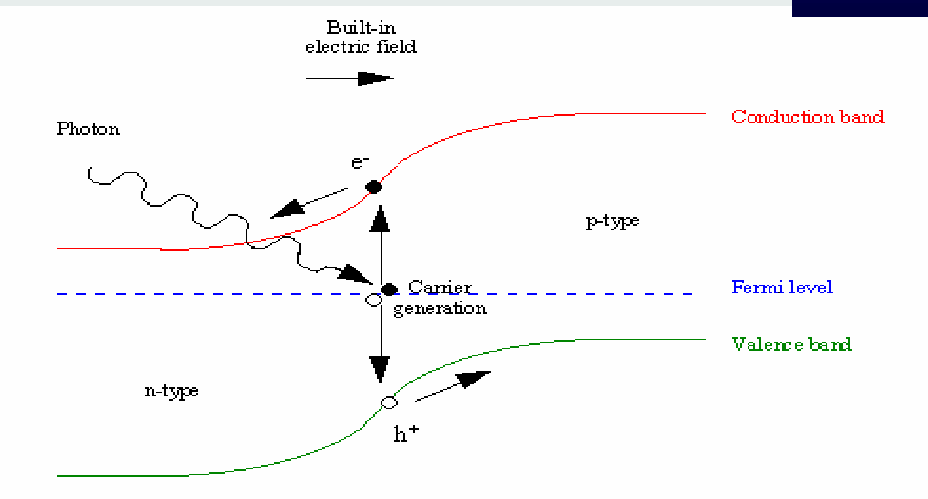

After Y. Wakchaure: _http://www.nd.edu/~gsnider/EE698A/Yogesh_Solar_cells.ppt

Efficiency Losses in Solar Cell

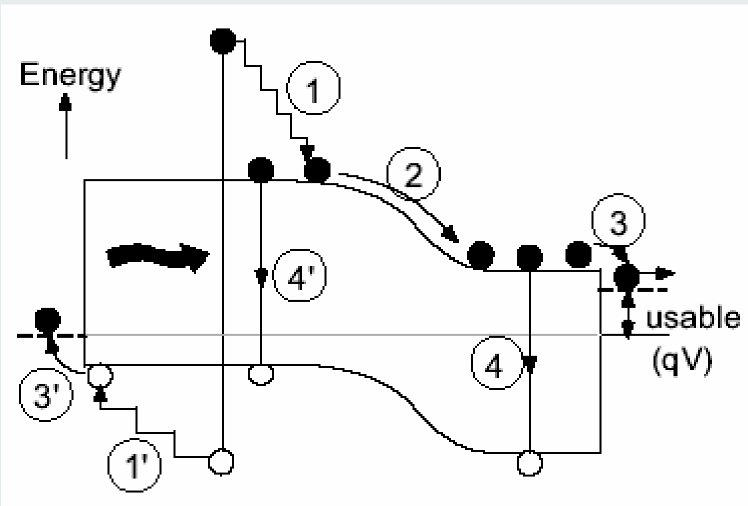

1 = Thermalization loss
2 and 3 = Junction and contact voltage loss
4 = Recombination loss

After Y. Wakchaure: _http://www.nd.edu/~gsnider/EE698A/Yogesh_Solar_cells.ppt

CdTe/CdS Solar Cell

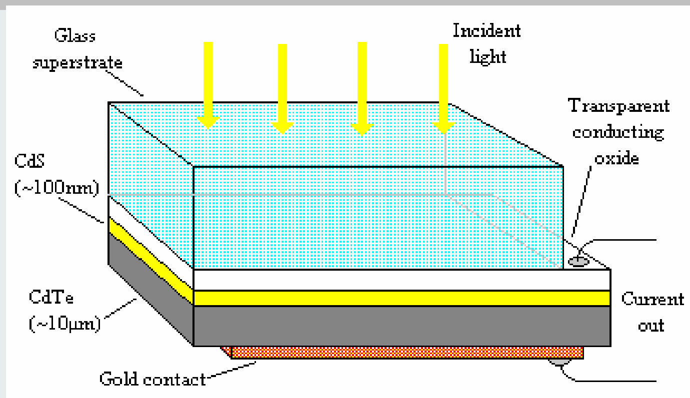

- CdTe : **Bandgap 1.5 eV; Absorption coefficient 10 times that of Si**
- CdS : **Bandgap 2.5 eV; Acts as window layer**

Limitation :

Poor contact quality with p-CdTe (~ 0.1 Ωcm²)

After Y. Wakchaure: _http://www.nd.edu/~gsnider/EE698A/Yogesh_Solar_cells.ppt

Solar Cells – Grätzel Cell

R. NESPER ETH ZÜRICH & COLLEGIUM HELVETICUM

Dye-Sensitized Solid-State Heterojunction Solar Cells

Michael Grätzel

The dye-sensitized solar cell (DSSC) provides a technically and economically viable alternative concept to present-day *p–n* junction photovoltaic devices. In contrast to conventional silicon systems, where the semiconductor assumes both the task of light absorption and charge carrier transport, these two functions are separated in DSSCs. The use of sensitizers having a broad absorption band in conjunction with wide-bandgap semiconductor films of mesoporous or nanocrystalline morphology permits harvesting a large fraction of sunlight. There are good prospects that these devices can attain the conversion efficiency of liquid-electrolyte-based dye-sensitized solar cells, which currently stands at 11%. In this article, we present the current state of the field, the realm of our review being restricted to the discussion of organic molecular hole conductors, which have demonstrated the best performance to date.

Solar Cell after M. Grätzel

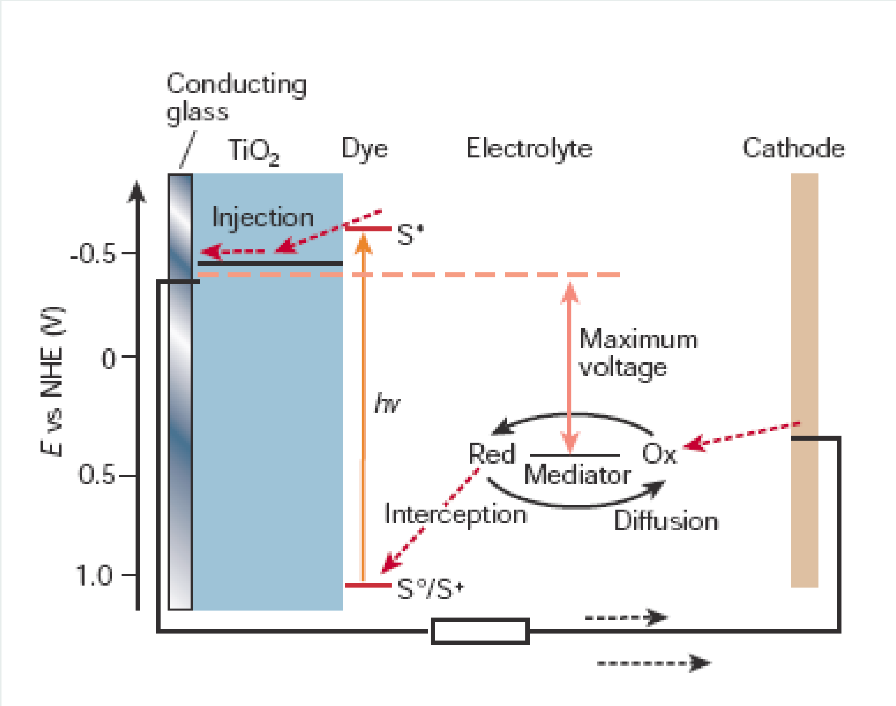

Grätzel Cell – Liquid Electrolyte - Working Principle

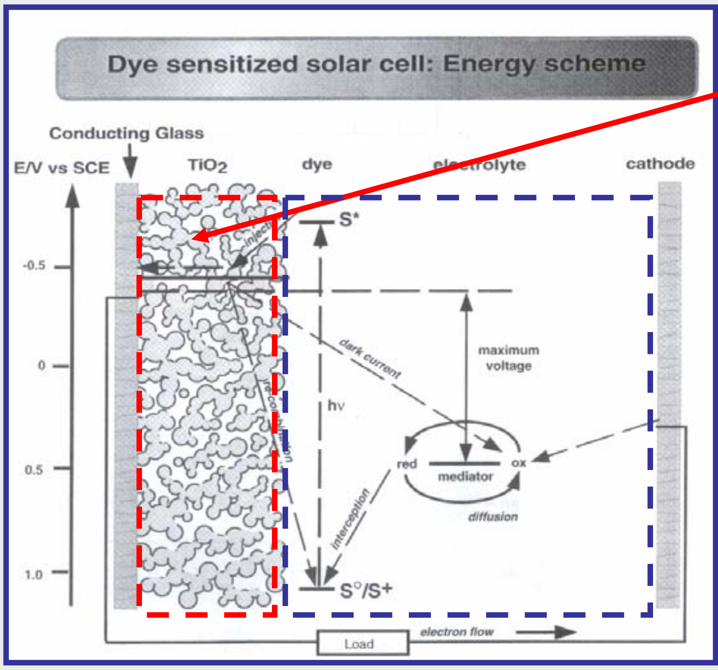

Nanoscopic TiO_2
– spherical particles

Electron excitation on dye
– Ru-complexes
– Ru^{2+} ➔ Ru^{3+}

Electron injection & conduction to electrode

– TiO_2 conduction band
– percolation through TiO_2 packing

Hole injection at dye
– $Ru^{3+} + I^-$ ➔ $Ru^{2+} + I$

Hole transport to cathode
– $I^- + I_2$ diffusion

cathode reaction
– $I_2 + 2e^-$ ➔ $2I^-$

Grätzel Cell – Electron Excitation - Dye

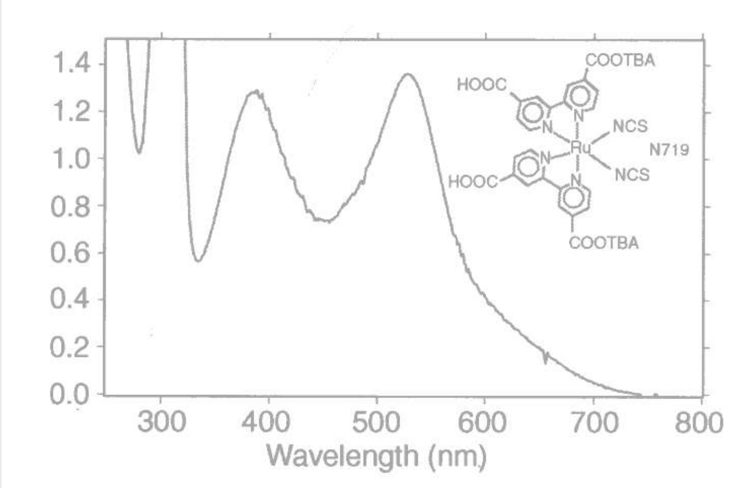

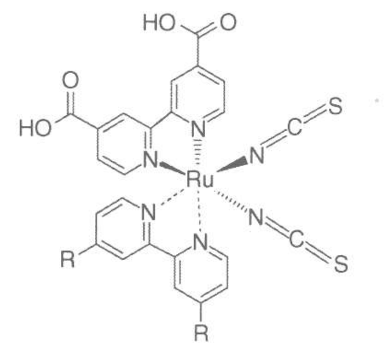

Electron excitation on dye ➔ MLCT type

Long alkyl chains extent into hydrophobic organic hole conductor

DSS Cell – Non-liquid Hole Conductor

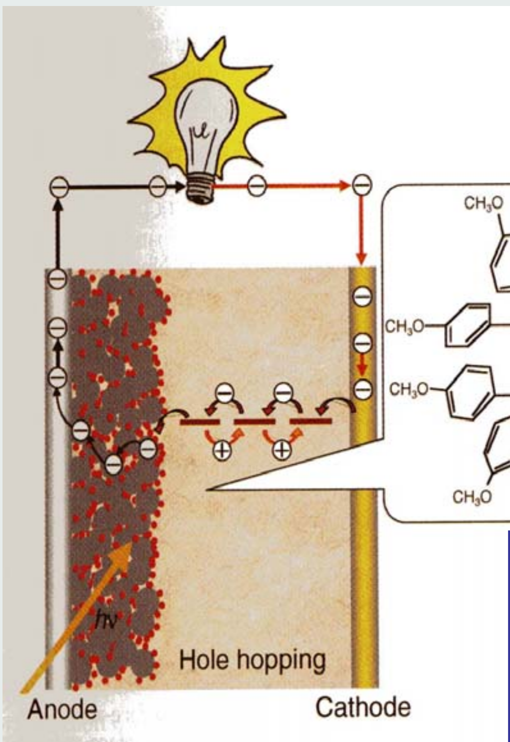

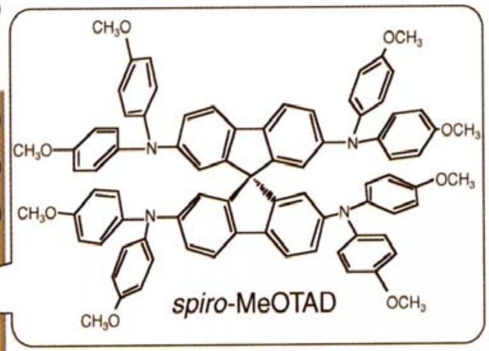

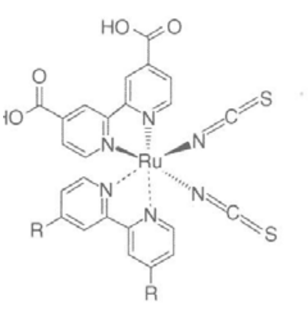

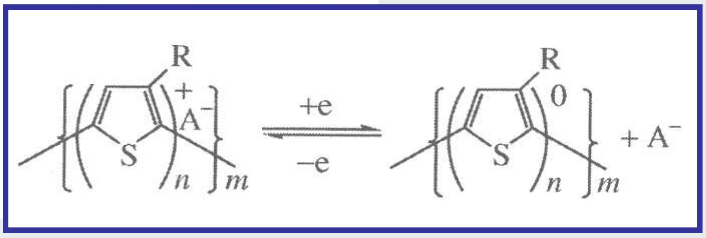

DSS-Cell – Time Scales – Loss Processes

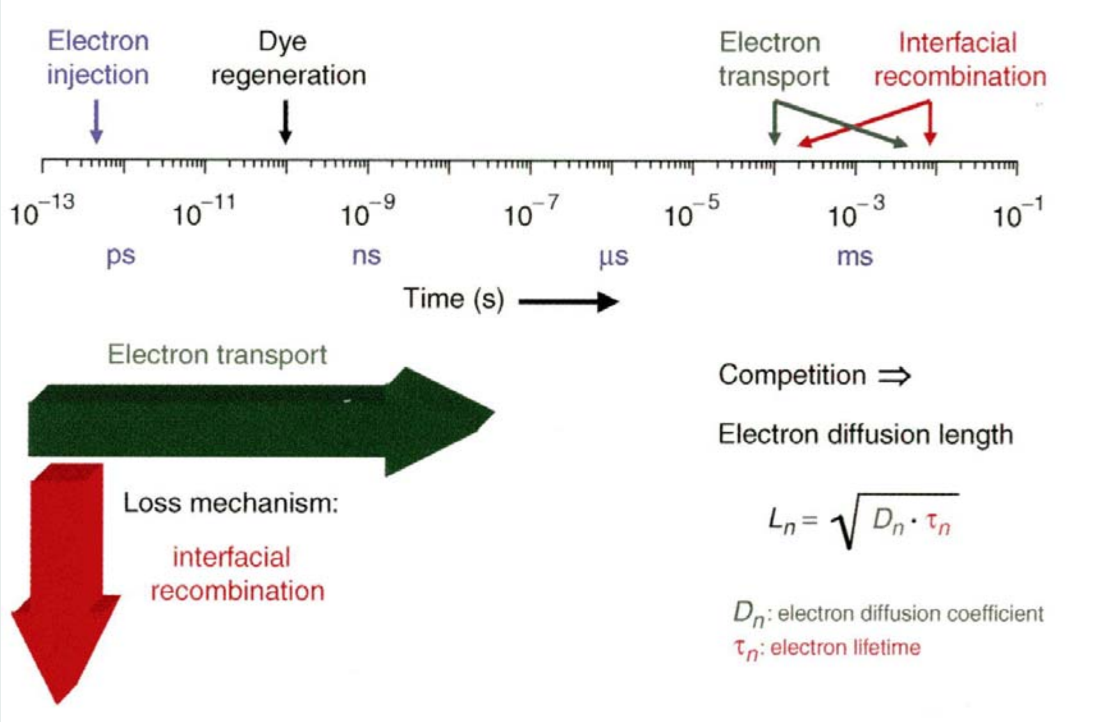

Grätzel Cell – Possible Enhancement

TiO_2 – Nano Fibers

energy conversion efficiency can rise to 33% in theory

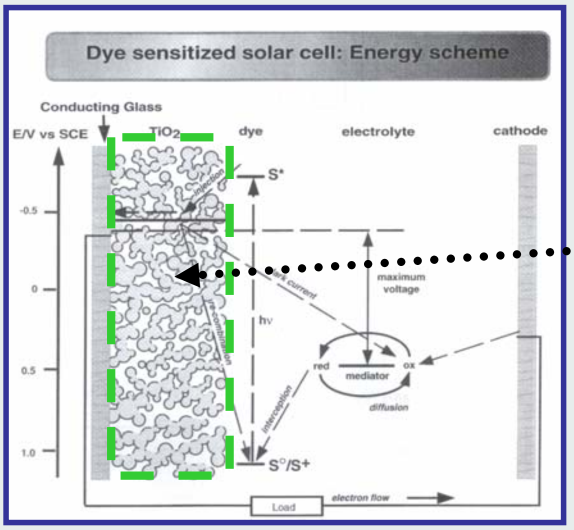

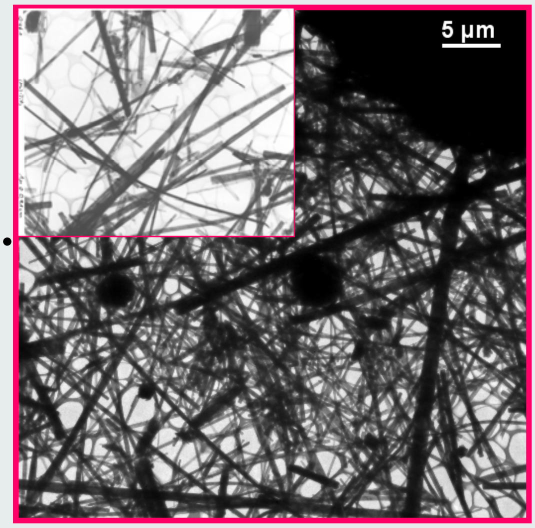

better percolation = higher efficiency

Tandem Cell for Water Cleavage

Based on two photosystems connected in series as shown in the electron flow diagram: A thin film of nanocrystalline tungsten trioxide, WO_3 (ref. 34), or Fe_2O_3 (ref. 35) serves as the top electrode absorbing the blue part of the solar spectrum. The valenceband holes (h+) created by band-gap excitation of the film oxidizewater to oxygen:

$$4h^+ + H_2O \Rightarrow O_2 + 4H^+$$

and the conduction-band electrons are fed into the second photosystem consisting of the dye-sensitized nanocrystalline TiO_2 cell discussed above. The latter is placed directly under the WO3 film, capturing the green and red part of the solar spectrum that is transmitted through the top electrode. The photovoltage generated by the second photosystem enables hydrogen to be generated by the conduction-band electrons.

$$4H^+ + 4e^- \Rightarrow 2H_2$$

The overall reaction corresponds to the splitting of water by visible light. There is close analogy to the 'Z-scheme' (named for the shape of the flow diagram) that operates in photosynthesis. In green plants, there are also two photosystems connected in series, one that oxidizes water to oxygen and the other generating the compound NADPH used in fixation of carbon dioxide.

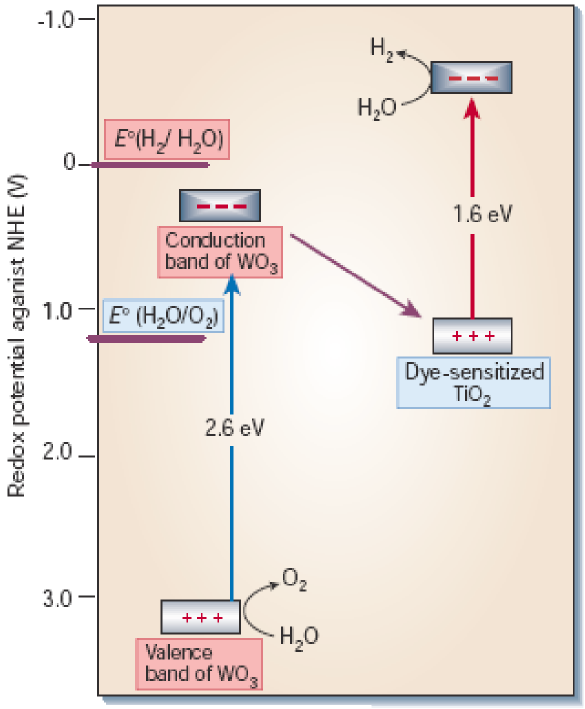

Grätzel, M. The artificial leaf, bio-mimetic photocatalysis. *Cattech* **3,** 3–17 (1999).

Silverclusters, Photography & Calzaferri Cell

Quantum-Sized Silver, Silver Chloride and Silver Sulfide Clusters

JOURNAL OF IMAGING SCIENCE AND TECHNOLOGY® • Volume 45, Number 4, July/August 2001

Gion Calzaferri▲, Dominik Brühwiler, Stephen Glaus, David Schürch, Antonio Currao, and Claudia Leiggener

$$[nAg^+, mAgCl] + \frac{r}{2}H_2O \xrightarrow{\text{light}} [(n-r)Ag^+, mAgCl, rAg^0] + rH^+ + \frac{r}{4}O_2 \qquad (1)$$

$$[(n-r)Ag^+, mAgCl, rAg^0] \xrightarrow{\text{electrode}} [nAg^+, mAgCl] + re^- \qquad (2)$$

$$Cl_2 + H_2O \rightarrow HOCl + H^+ + Cl^- \qquad (5)$$

$$2HOCl \xrightarrow{Ag^+} O_2 + 2H^+ + 2Cl^- \qquad (6)$$

$$[AgCl]Ag_s^+ \xrightarrow{\text{light}} [AgCl]\{Ag^+, Ag^0\}_{s,i} + Cl_s^\bullet \qquad (3)$$

The $Cl_s^\bullet$ radicals recombine very fast to form Cl_2:

$$2Cl_s^\bullet \rightarrow Cl_2 \qquad (4)$$

$$Ag^0 + Ag_r^{q+} \rightarrow Ag_{(r+1)}^{q+} \qquad (r \geq 1;\ 0 \leq q \leq r) \qquad (7)$$

Silverclusters and Solar Conversion

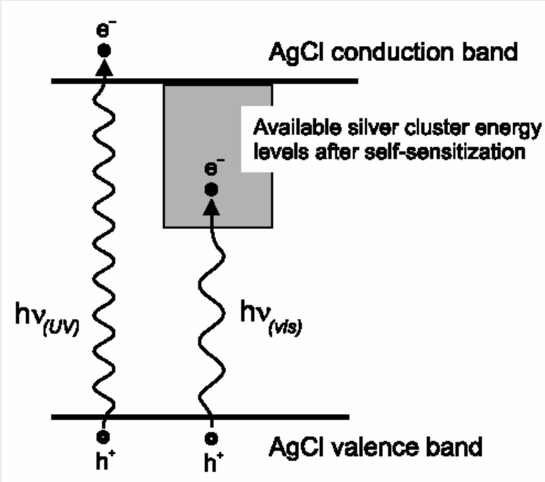

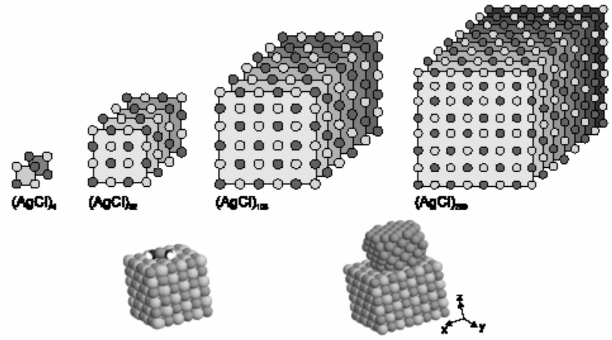

Figure 4. Clusters and composites discussed in this article. Top: $(AgCl)_n$ clusters with (100) surfaces. Bottom left: the composite $(Ag)_{115}(AgCl)_{192}$. Bottom right: an adsorbed $Ag^{+}(H_2O)_2$ on the surface of $(AgCl)_{108}$.

$$Ag^0 + Ag_r^{q+} \rightarrow Ag_{(r+1)}^{q+} \qquad (r \geq 1;\ 0 \leq q \leq r) \qquad (7)$$

$$Cl_2 + H_2O \longrightarrow HOCl + H^+ + Cl^- \qquad (5)$$

$$2HOCl \xrightarrow{Ag^+} O_2 + 2H^+ + 2Cl^- \qquad (6)$$

Silverclusters and Solar Conversion

R. NESPER ETH ZÜRICH & COLLEGIUM HELVETICUM

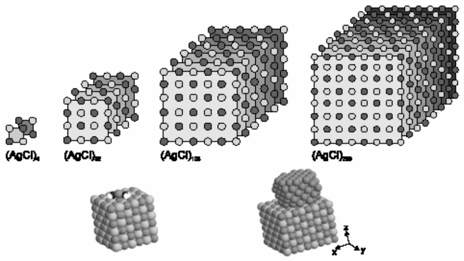

Figure 4. Clusters and composites discussed in this article. Top: $(AgCl)_n$ clusters with (100) surfaces. Bottom left: the composite $(Ag)_{115}(AgCl)_{192}$. Bottom right: an adsorbed $Ag^{+}(H_2O)_2$ on the surface of $(AgCl)_{108}$.

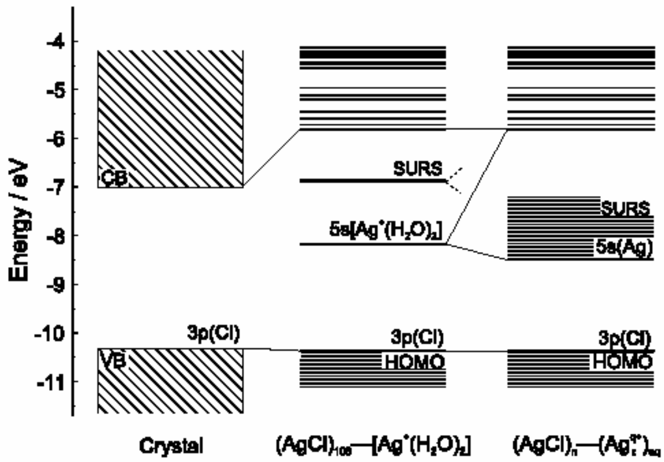

Figure 5. Comparison of the electronic structure of a silver chloride crystal, a silver chloride nanocluster with one $Ag^{+}(H_2O)_2$ adsorbed on its surface, and one with several of them adsorbed (some of them already reduced and therefore represented as $(Ag_r^{q+})_{aq}$). The crystal band gap and $(AgCl)_n$–$(Ag_r^{q+})_{aq}$ values correspond to experimental results.

$$Ag^0 + Ag_r^{q+} \rightarrow Ag_{(r+1)}^{q+} \qquad (r \geq 1;\ 0 \leq q \leq r) \qquad (7)$$

$$Cl_2 + H_2O \longrightarrow HOCl + H^+ + Cl^- \qquad (5)$$

$$2HOCl \xrightarrow{Ag^+} O_2 + 2H^+ + 2Cl^- \qquad (6)$$

Silverclusters and Solar Conversion

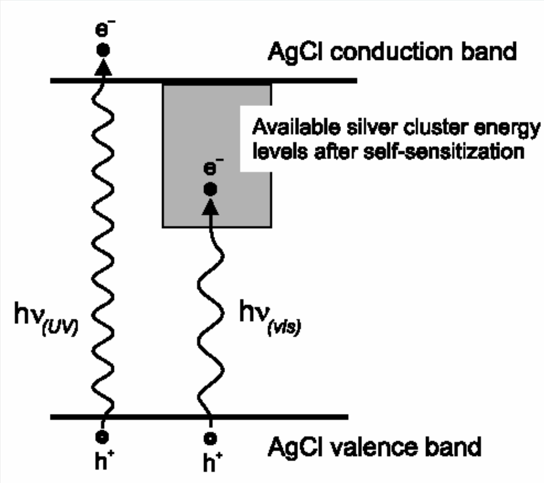

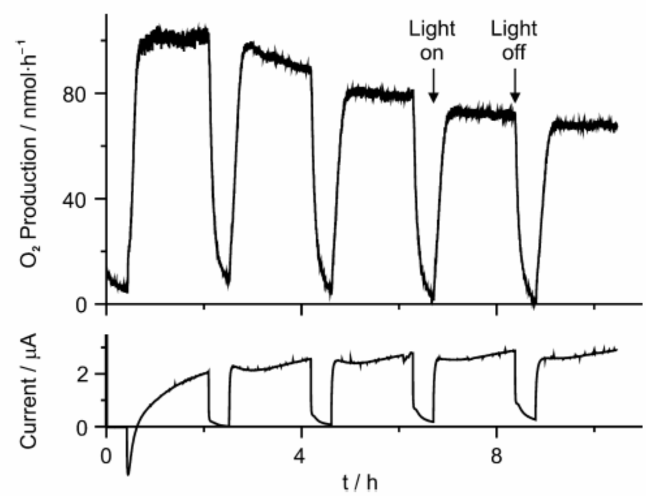

Figure 2. Chronoamperometry of a AgCl-coated SnO_2:F electrode, carried out at 0.64 V versus NHE, with illumination and dark periods. The O_2 production rate (nmol·h^{-1}) and the photocurrent (µA; anodic current is drawn upwards) are plotted versus time.[9]

$$Ag^0 + Ag_r^{q+} \rightarrow Ag_{(r+1)}^{q+} \qquad (r \geq 1;\ 0 \leq q \leq r) \qquad (7)$$

Two-Photon Solar Conversion System

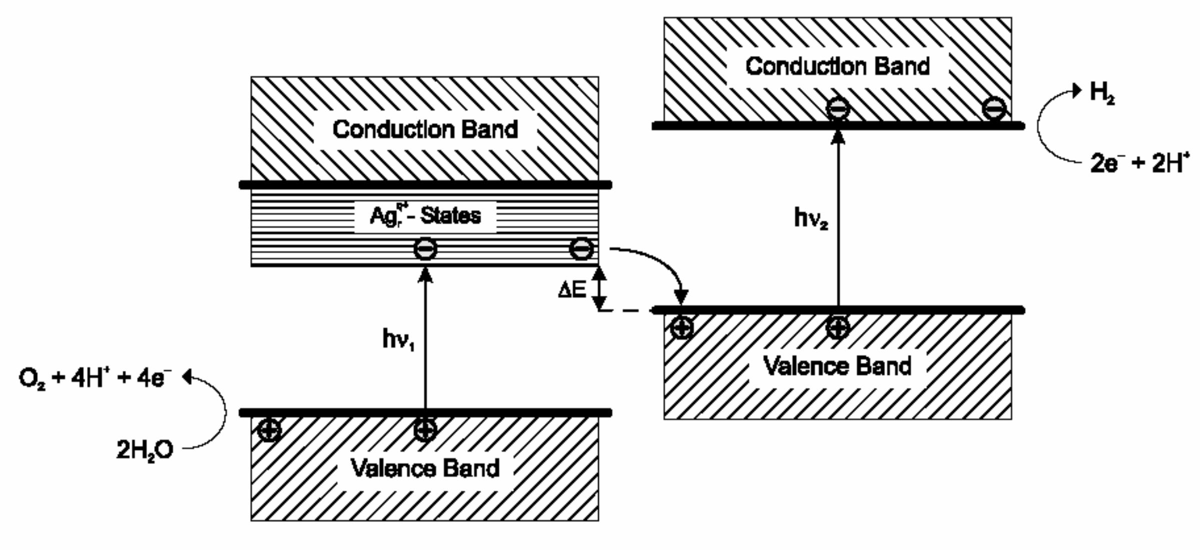

Flexible Thin Film Cells

Flexible CIGS solar cells
ZnO:Al/ZnO/CdS/CIGS on 10 x 10 cm² polyimide

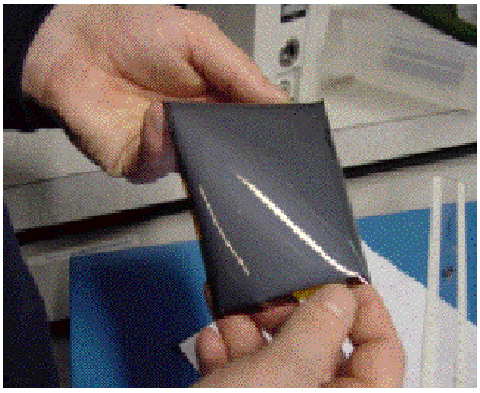

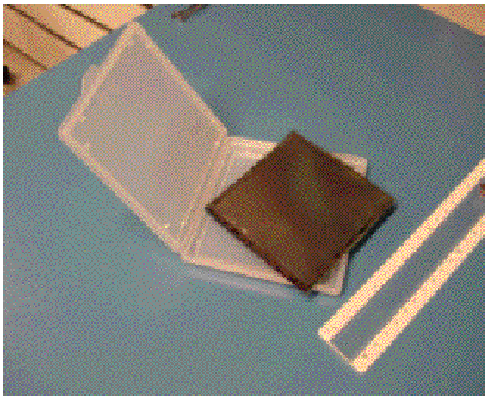

Deposition possible on 15 x 15 cm² polyimide

Further development

Scribing, process optimization, connections, encapsulation

Flexible Thin Film Cells

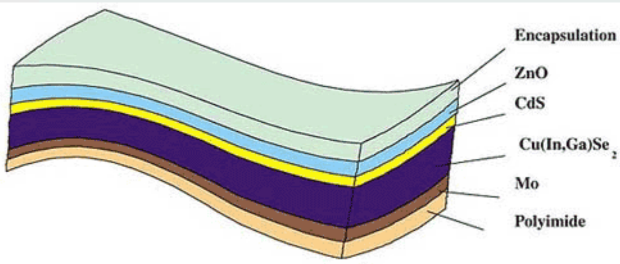

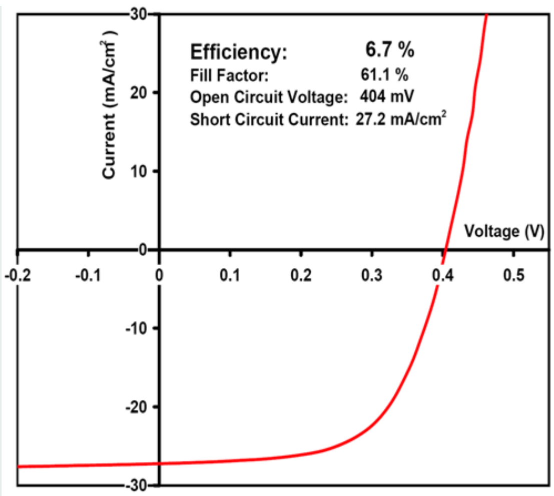

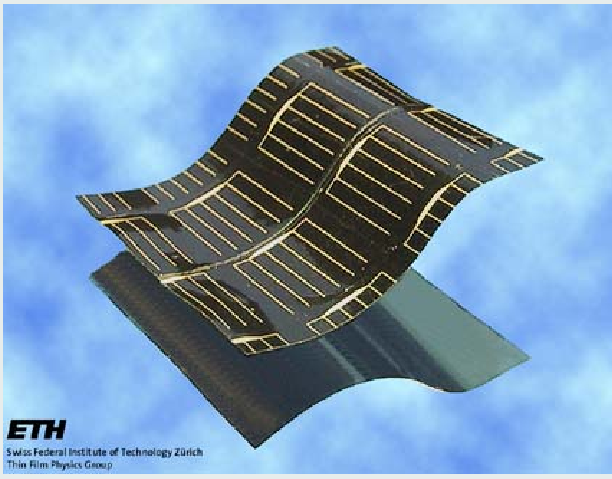

Multiband Cells

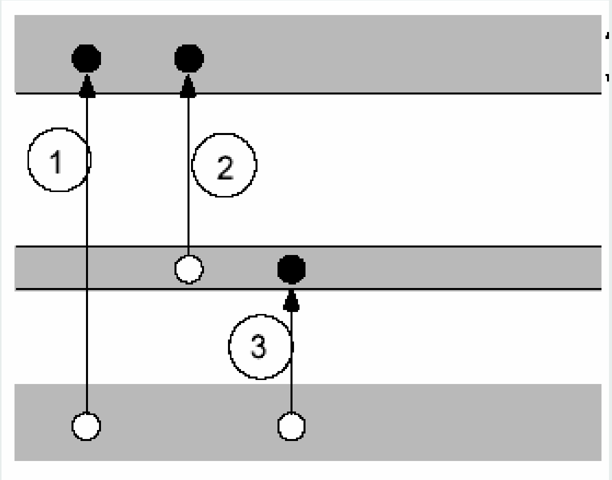

- **Intermediate band formed by impurity levels.**
- **Process 3 also assisted by phonons**
- **Limiting efficiency is 86.8%**

Thermophotovoltaic Cell

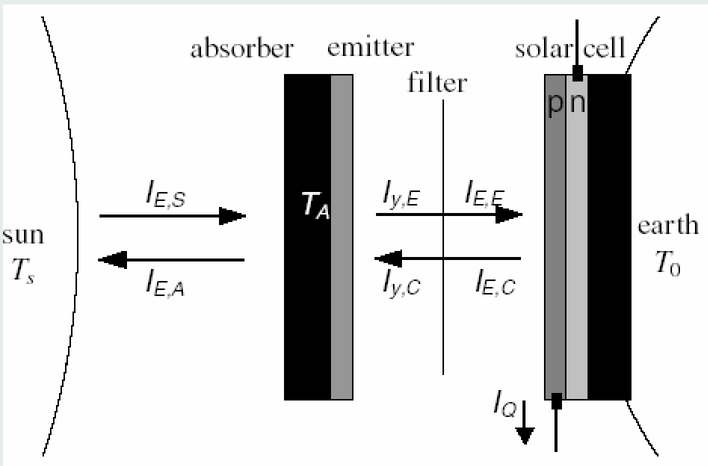

Burner:-
Burns fuel and heats up the emitter.
Emitter:-
Emits radiant heat energy.
Filter:-
Selectively allows suitable radiation through to the PhotoVoltaic cell.
The remaining radiation is reflected back to the emitter to maintain the temperature and improve efficiency.
Thermophotovoltaic cell:-
the radiation incident on the cell causes a potential across the cell, just like in a solar cell but with heat radiation.

- **Filter passes radiations of energy equal to bandgap of solar cell material**
- **Emitter radiation matched with spectral sensitivity of cell**
- **High Illumination Intensity (~ 10 kW/m^2)**

Thermophotovoltaic Cells

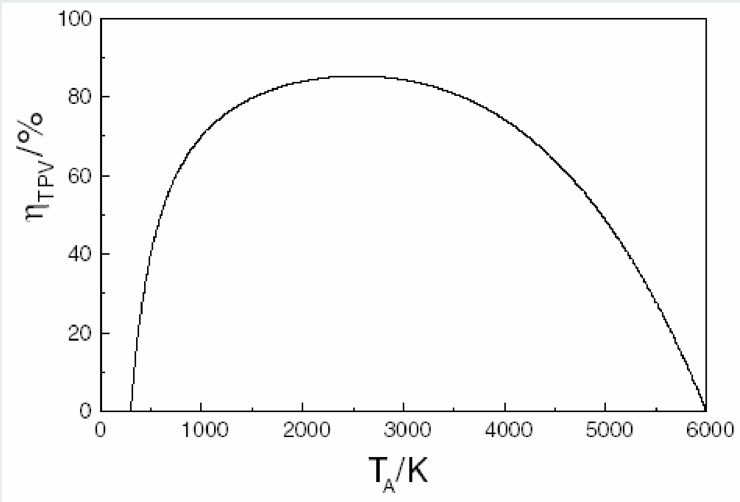

$$\eta_{\mathrm{TPV}} = \left(1 - \frac{\pi}{\Omega_S}\frac{T_A^4}{T_S^4}\right)\left(1 - \frac{T_0}{T_A}\right)$$

- Efficiency almost twice of ordinary photocell

Present State of Cell Development

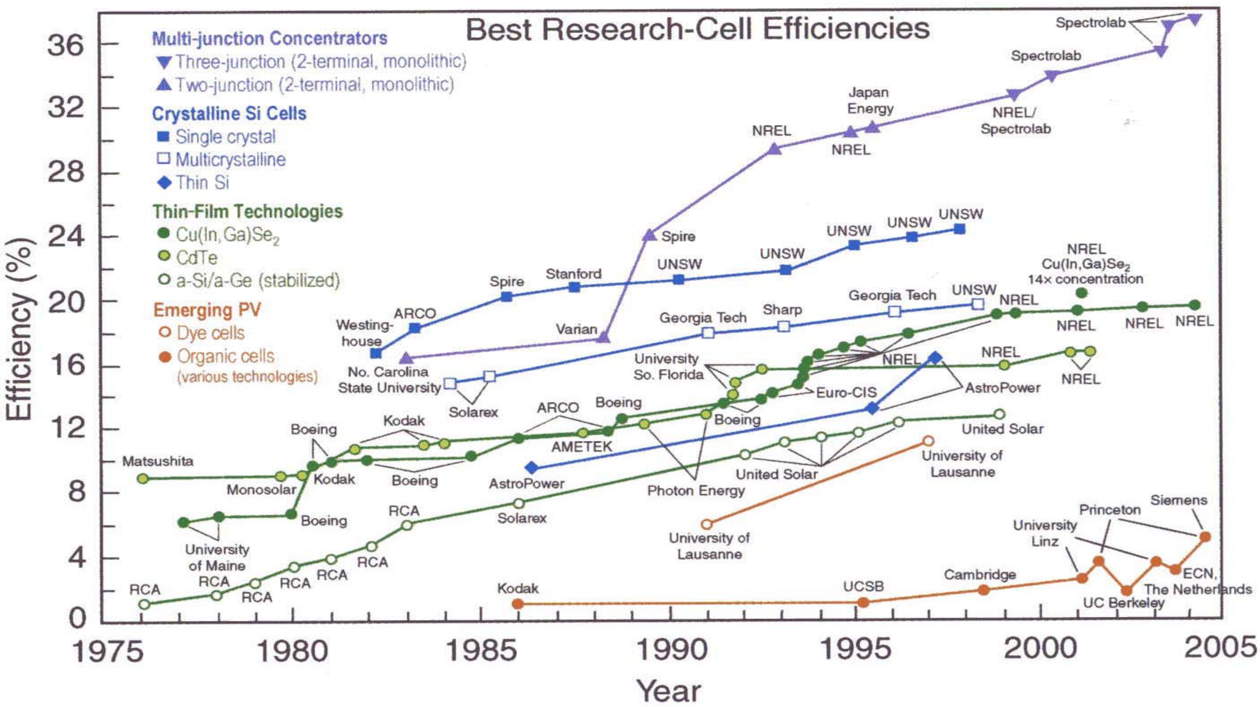

Searching New Materials for Energy Conversion and Energy Storage

R. NESPER ETH ZÜRICH & COLLEGIUM HELVETICUM

1. Renewable Energy
2. Solar Cells
3. **Thermoelectricity**
4. Fast High Energy Li-Ion Batteries
5. Light Emitting Devices
6. Hydrogen Storage
7. Luminescent Materials
8. New Materials

Thermo-Electricity

R. NESPER ETH ZÜRICH & COLLEGIUM HELVETICUM

1. Generation of Thermoelectricity
2. Thermoelectric Cooling – Peltier effect

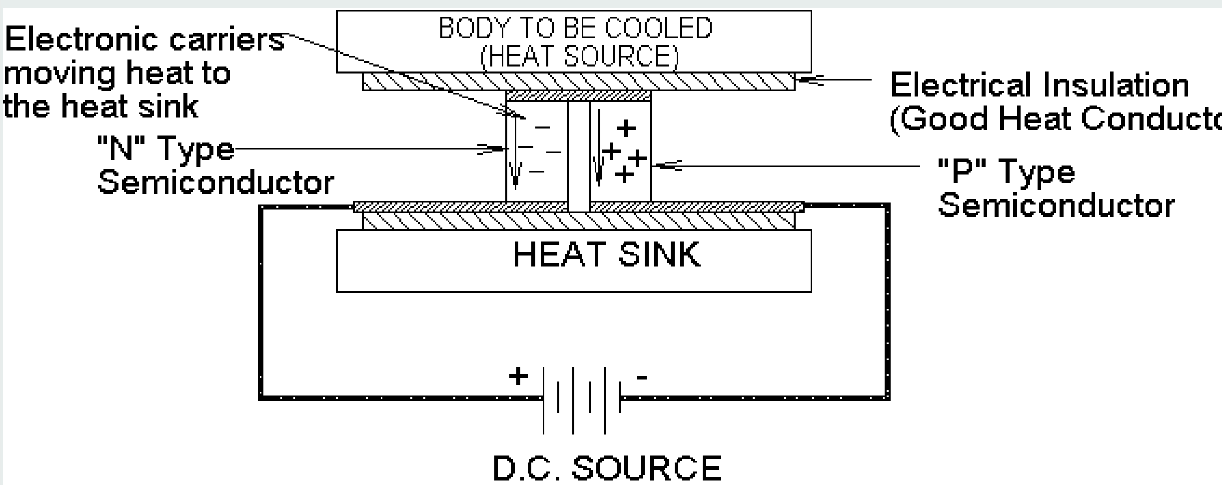

Prerequisites for Good Thermoelectric Materials

1. **Semiconductor**
2. **Low carrier concentration**
3. **High Carrier Mobility**
4. **Low Thermal conductivity**

1. **Right band gap**
2. **Bad thermal conductor**
3. **Good electronic conductor**
4. **Scatter lattice vibration**

$$zT = \alpha^2 / (\kappa\rho)$$

κ = heat conductivity

ρ = heat conductivity

α = Seebeck coefficient

Table 1. The maximum efficiencies η_m calculated using different methods.

	Units	I	II	III
T_c	K	400	400	400
T_h	K	75 0	1500	1500
ρ	Ω cm	0.04	$1/T$	0.001
α	μV/K	$211+0.15T$	200	$0.2T$
k	W/(cmK)	$3.194/T$	$10/T$	$3/T$
Linear solution				
J_m	A/cm²	−1.23	−67	−47
η_m		0.031	0.34	0.48
ZT		0.23	3.43	10.9
Numerical solution				
J_m	A/cm²	−1.23	−59	−31
η_m		0.030	0.28	0.39
Our solution				
J_m	A/cm²	1.234	58.20	32.15
η_m		0.02993	0.2857	0.3920

Thermo-Electricity - Principle

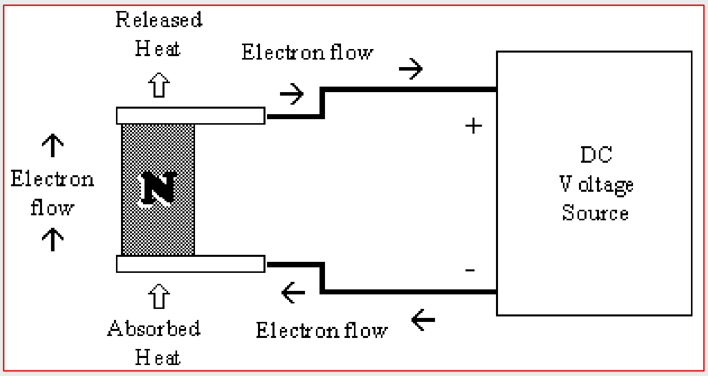

n- type semiconductor

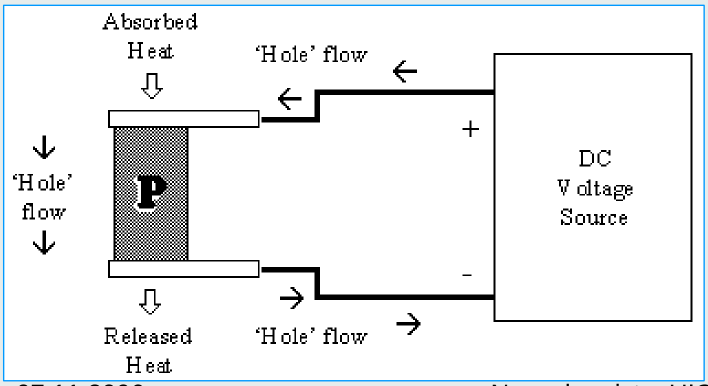

p- type semiconductor

Thermo-Electricity - Principle

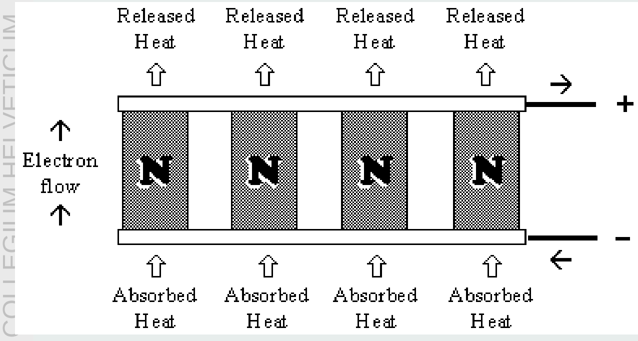

High current – low voltage

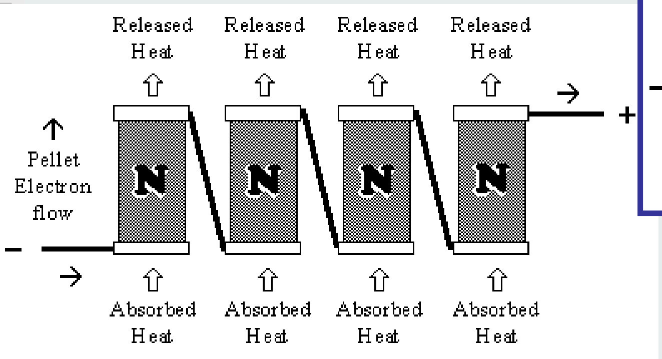

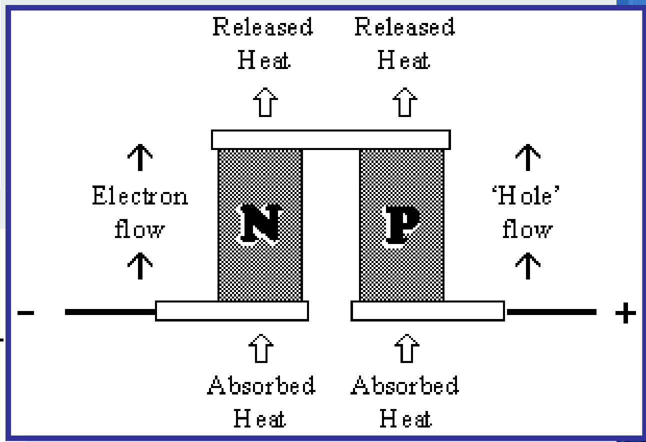

Contact heating

Thermo-Electricity - Materials

1. Generation of Thermoelectricity
2. Thermoelectric Cooling

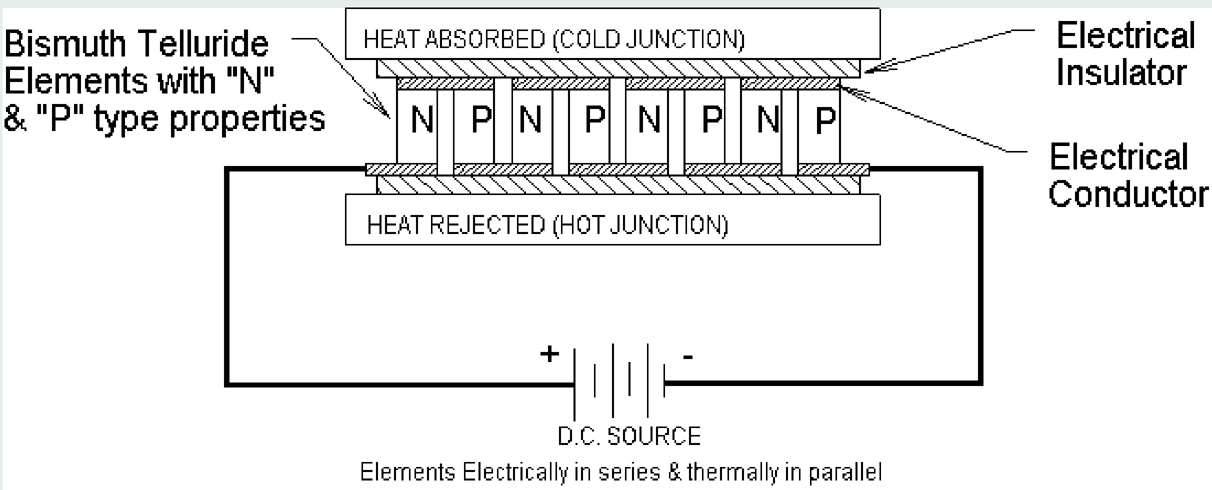

Thermo-Electric Devices

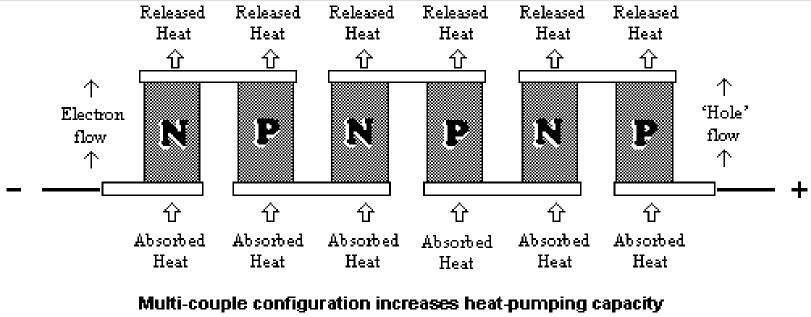

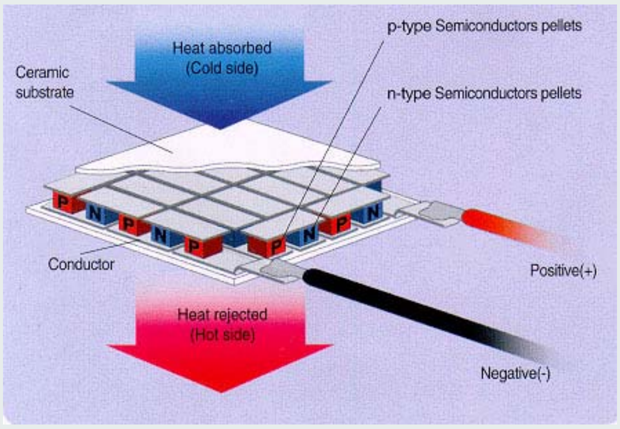

High voltage - low current

Thermo-Electric Devices

electricity ➔ cool
electricity ➔ heat

Can Thermoelectric systems be used for heating as well?
Yes. One of the benefits of TE technology is that you can switch the direction of heat pumping by simply reversing the polarity of the applied voltage—you get heating with one polarity, cooling with the other. Thermoelectric modules make very efficient heaters—in fact, because of the unique properties of Peltier devices, any given TE system will have a greater capacity for heating a load than cooling it.

What type of products currently use this technology?
There are an increasing number and variety of products which use thermoelectric technology—from picnic boxes to water coolers, laser applications, and highly-specialized instrumentation and testing equipment. The compatibility of many TE's with automotive voltages, makes them especially suitable for small cooling jobs in that industry.

For heat-only applications, do thermoelectric devices have advantages over resistive heaters?
Yes. Resistive devices create heat solely by virtue of the power dissipated within them. TE devices, on the other hand, not only provide this I 2R heating, but also actively pump heat into the thermal load; this, potentially, makes them much more efficient than resistive heaters.

Thermo-Electric Devices

R. NESPER ETH ZÜRICH & COLLEGIUM HELVETICUM

Δ T ➔ electricity

Nanostructured Thermoelectric Devices May Generate Power from Thermal Sources

A car's engine loses 70 percent of its energy as waste heat
➔ a way not only to recover that lost energy
➔ capture the power-producing potential of geothermal heat

Thermoelectric materials try to recover this energy by converting it to electricity, but they don't work very well if the flow of heat is uncontrolled.

➔ breakthrough involves controlling the motion of electrons using materials that are structured on the nanoscale.

Nanostructured Thermoelectric Devices May Generate Power from Thermal Sources

R. NESPER ETH ZÜRICH & COLLEGIUM HELVETICUM

Δ T ➔ electricity

if an electrical voltage is applied to an electrical system in addition to a temperature difference, it is possible to harness electrons having a specific energy.

Nanostructured Thermoelectric Devices May Generate Power from Thermal Sources

Δ T ➔ electricity

➔ if an electrical voltage is applied to an electrical system in addition to a temperature difference, it is possible to harness electrons having a specific energy.

This means that if a nanostructured material is designed to only allow electrons with this particular energy to flow, a novel type of equilibrium is achieved in which electrons do not spontaneously ferry heat from hot to cold.

Until now, the efficiency of such devices, which have no moving parts and can be small enough to fit on a microchip, has been too low (less than 15 percent of the Carnot limit for power generation) for use in all but a few specialized applications.

However, tailoring the electronic bandstructure in state-of-the-art thermoelectric materials made up of a huge number of nanowires.
If all goes well, nanostructured thermoelectric devices with efficiencies close to 50 percent of the Carnot limit may be realized.

Nanostructured highly effective Thermoelectrics

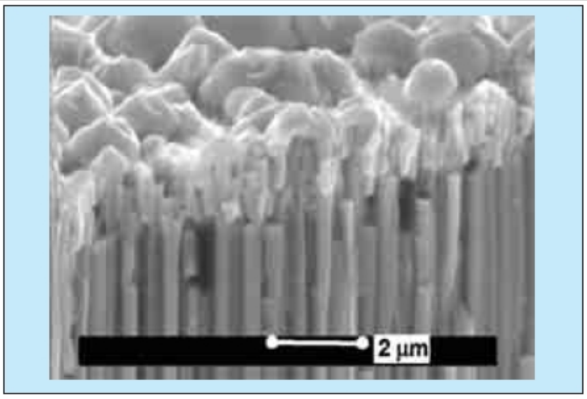

Figure 1. Thermoelectric Nanowires of n-Type Bi_2Te_3 with a diameter of 10 nm and length of 40 µm were grown in an alumina template. The thermoelectric material was allowed to grow onto the top of the template, forming caps that make contact with each other. In a production version, the overgrowth and part of the template would be polished away and metal contacts deposited as in Figure 2.

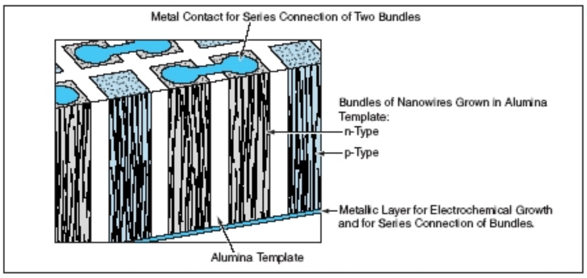

Figure 2. Bundles of Nanowires would be grown electrochemically in an alumina template. The nanowires in each bundle would be electrically connected in parallel and the bundles electrically connected in series by metal contacts grown electrochemically on the ends of the bundles.

fabricated by electrochemical growth

may contain nearly a billion elements (wires) per square centimeter

Nanowires have been grown in alumina templates with pore diameters of 100 and 40 nm

The predicted net effect of reducing diameters to the order of tens of nanometers would be to increase its efficiency by a factor of 3

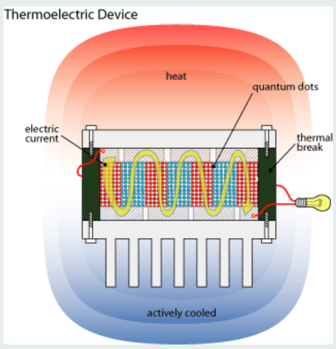

(Nanostructured) Highly Effective Thermoelectrics

R. NESPER ETH ZÜRICH & COLLEGIUM HELVETICUM

Δ T ➔ electricity

Skutterudites - (Co,Ni)As_{3-x}

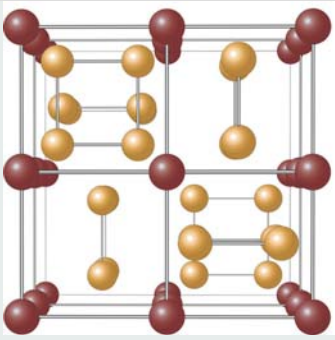

Clathrates

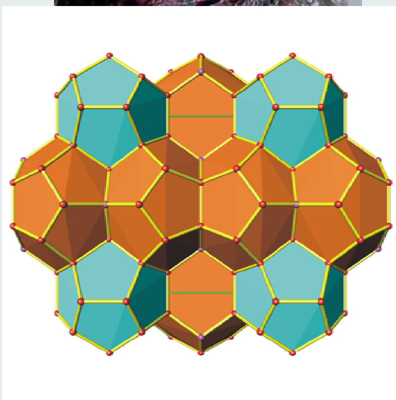

Zinkantimonide

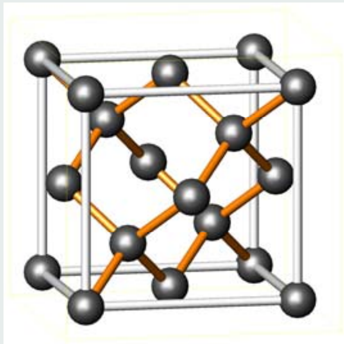

Renewable Energy Cycle - II

R. NESPER ETH ZÜRICH & COLLEGIUM HELVETICUM

- **solar energy**
- **no extra carbon dioxide evolution**
- **low temperature burning**

- **Solar conversion**
- **Energy storage**
- **Energy uses**

1. Solar Cell

(a) $2H_2O \longrightarrow 2H_2 + O_2$ +572 kJ/mol
(b) electric current

2. Fuel cell combustion

$2H_2 + O_2 \longrightarrow 2H_2O$ -572 kJ/mol

Searching New Materials for Energy Conversion and Energy Storage

1. Renewable Energy
2. Solar Cells
3. Thermoelectricity
4. **Fast High Energy Li-Ion Batteries**
5. Light Emitting Devices
6. Hydrogen Storage
7. Luminescent Materials
8. New Materials

Batteries, Supercaps & Fuel Cells

Ragone-Diagramm

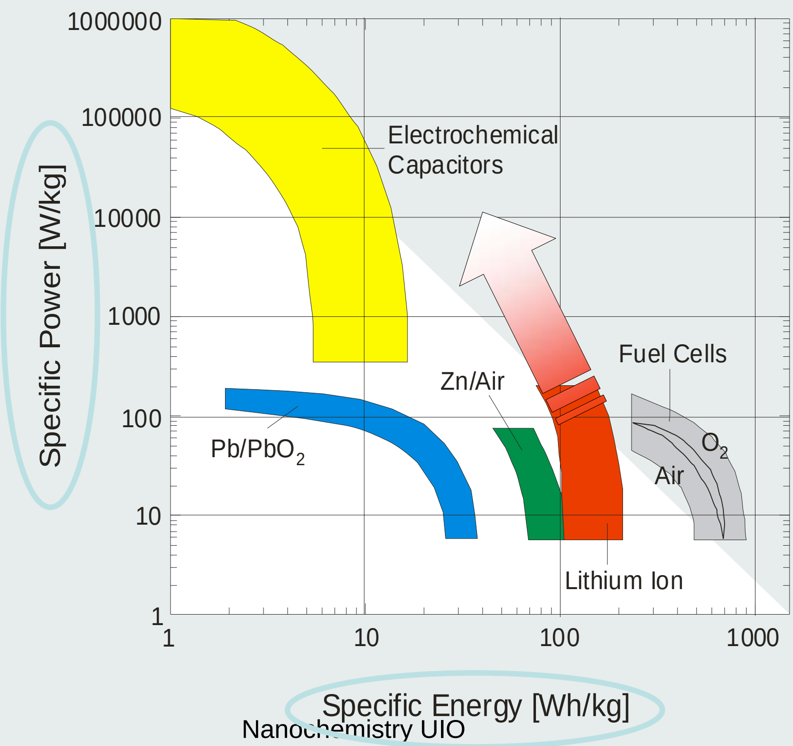

electrochemical cells

Charakteristics of electrochemical cells

Spezific Charge: $Q = zF/\sum_n M_n \quad [Ah/kg]$

$Q_v = Q \cdot \rho \quad [Ah/l] \quad (\rho = \text{Density in kg/l})$

Spezific Energy: $W = UQ = \frac{U \cdot z \cdot F}{\sum_n M_n} = -\frac{\Delta G}{\sum_n M_n} \quad [Wh/kg]$

Spezific Power: $P = \frac{U \cdot i}{\sum_n m_n} \quad [W/kg]$

Batteries Systems

Some important battery systems

	Anode (-)	Elektrolyt (Diaphragma)	Kathode (+)	
1.2 - 2 V Systeme, wässerige Systeme	Pb	H_2SO_4	PbO_2	~ 30 - 50 Wh/kg
	Cd	KOH	NiOOH	
	MeH_x	KOH	NiOOH	~ 50 - 80 Wh/kg
	Zn	KOH	NiOOH	
	Zn	KOH	MnO_2	
	H_2	KOH	NiOOH	
	Zn	ZnBr, KBr	Br_2 - Komplex	
	Zn	KOH	O_2	
2 - 4 V Systeme, Aprotische Elektrolyte oder Festelektrolyte	Na	b-Al_2O_3	S_x	~ 80 - 120 Wh/kg
	Na	b-Al_2O_3, $NaAlClO_4$	$NiCl_2$	
	Li	aprot. Lösungsmittel + Salz	MeO_x	
	Li	Polyäther + Salz	MeO_x	
	Li	Polyäther + Salz	Thio-org. Verb.	

Battery with Porous Electrodes

Lithium ion battery

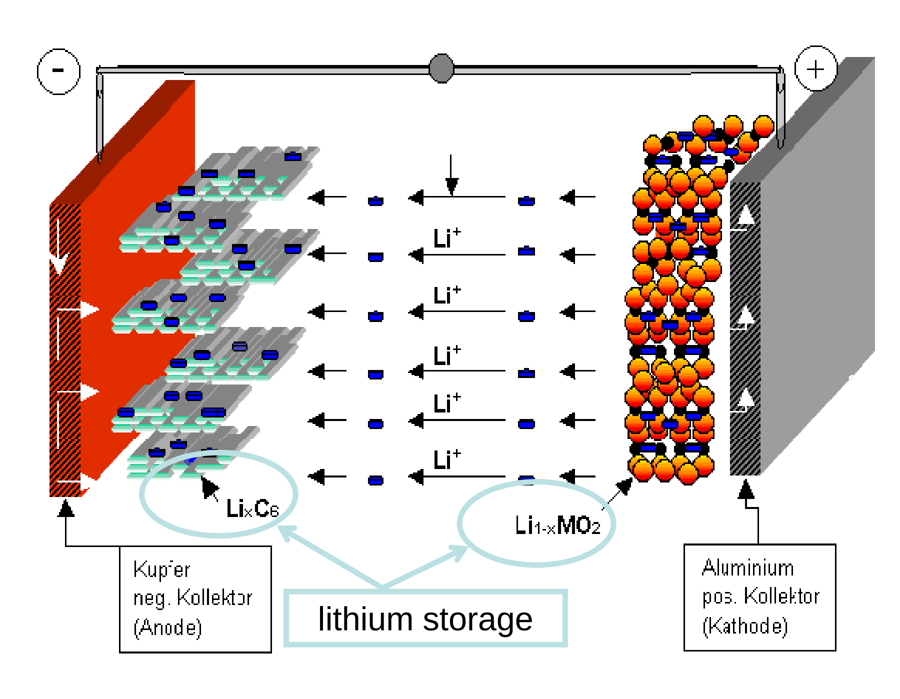

Batteries & Potentials

electrochemical potentials of different electrode materials

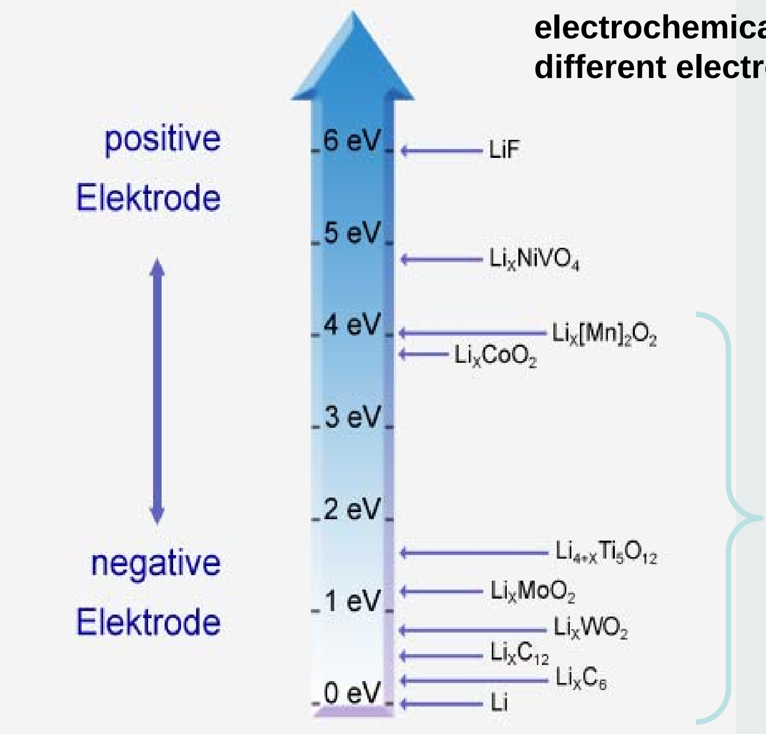

lithium ion battery

$$U = \Delta E \approx 4V$$

Lithium-Ion Battery - Components

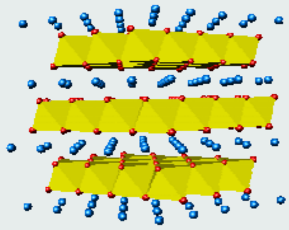

Cathode : Transition metal oxide T (Li_xTO_2)

Working x: 0 < x < 0.5

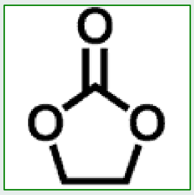

Electrolyte: 1,3-Dioxolan-2-one (ethylen carbonate) / $LiClO_4$ oder $LiPF_6$

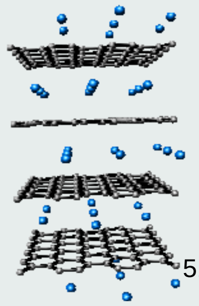

Anode: Graphite (Li_yC_6)

Working x: 0 < x < 1

1. Fast High Energy Li-Ion Batteries

Why aren‘t there Li-Ion batteries in handheld working tools ?
Why aren‘t there Li-Ion batteries in electric cars?

Full Batteries:

1. **Optimized for specific energy: ca. 160 Wh/kg at C/3**
2. **Optimized for specific power: ca. 60 Wh/kg at 20C**
3. **Optimization for spec. energy & spec. power ???**

Basically,the cathodes are kinetically slow at a reasonable reversible capacity.

Possible Electrodes

R. NESPER ETH ZÜRICH & COLLEGIUM HELVETICUM

Anodes are not the fundamental problem

1. Optimal electro-active material : Anode

Graphite	**1500 Wh/kg at 20C**
Tetrel alloys (stannides)	**~2000 Wh/kg at 10C [1]**
TiO_x spinels	**500 Wh/kg at 12C [2]**

[1] Chen,Chevrier, Christensen, Dahn, Electrochem. Solid-State Lett., 2004, 7, A310-A314
[2] CHRISTENSEN, SRINIVASAN, NEWMAN, J. Electrochem. Soc. **2006,** 153, A560

Presently cells suitable for hand-held machines and cars [3]

Lead	**40 Wh/kg**
Ni-Cd	**50 Wh/kg**
Ni-MH	**70 Wh/kg**

[3] Trueb, Rueschi, Batterien & Akkumulatoren, Springer 1998

Nanocrystalline Anatase-Fibers

R. NESPER ETH ZÜRICH & COLLEGIUM HELVETICUM

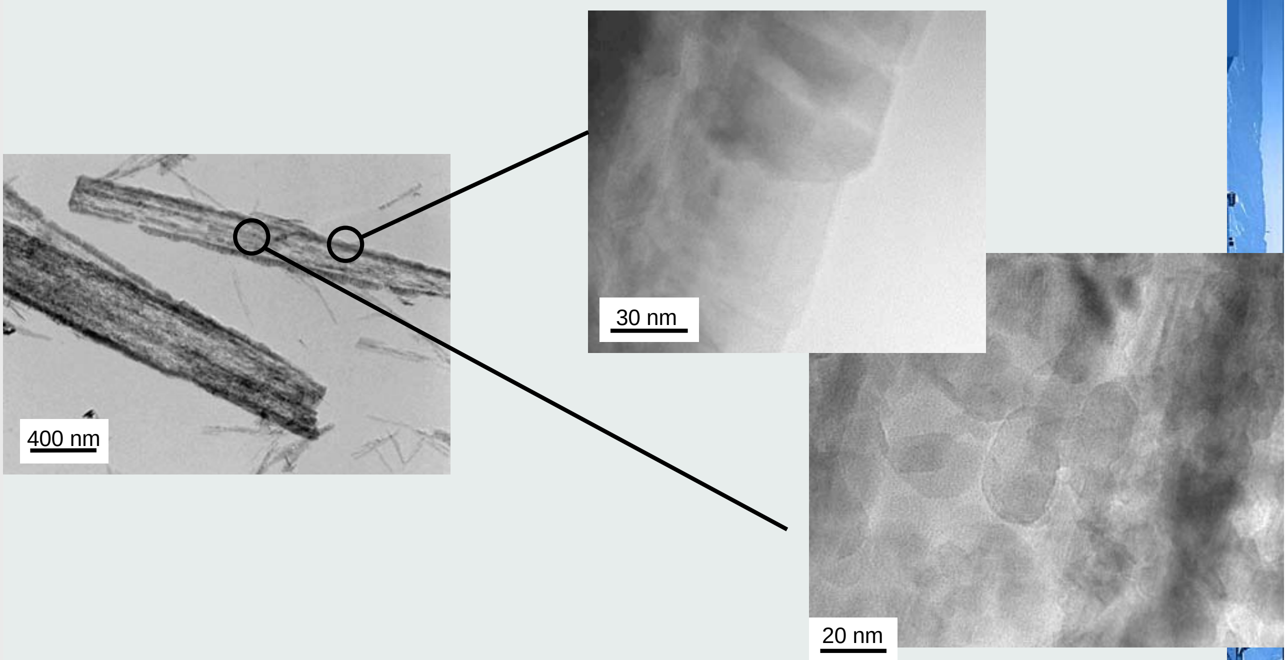

TiO2-Nano Fibers in Thin Film Electrodes

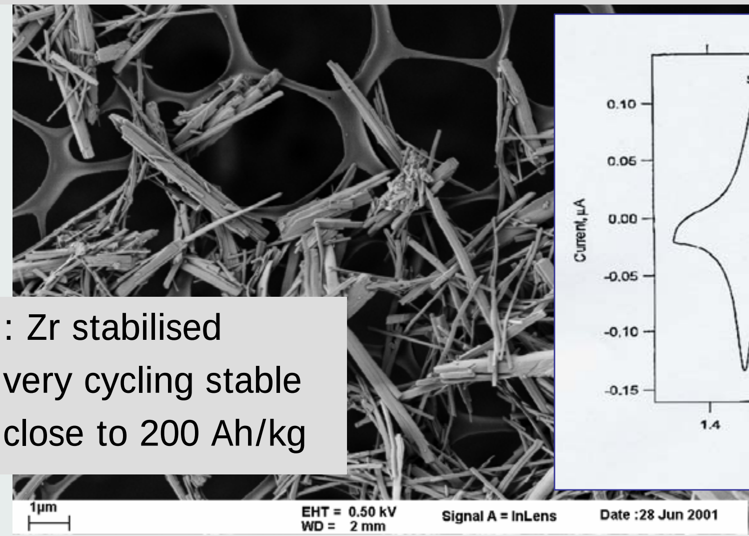

TiO_2 : Zr stabilised
- very cycling stable
- close to 200 Ah/kg

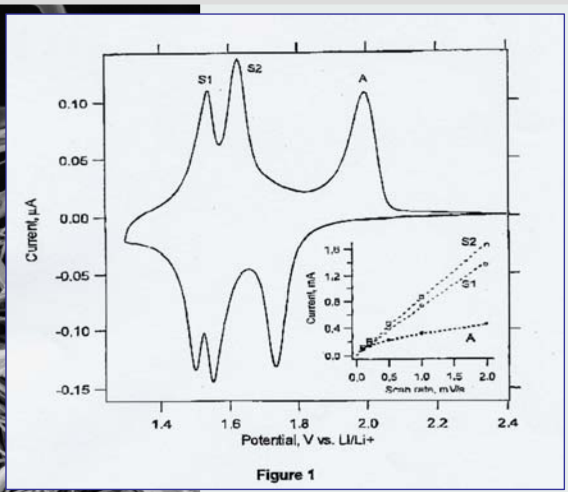

Integral voltammetric charge from the anodic branch of cyclic voltammograms is plotted as a function of scan rate. The charge was normalized against the charge-capacity of the same electrode at the slowest scan (0.1 mV/s). Open points: material N11, squares: material N12, triangles: material N9. Full points + dashed line: reference non-organized nanocrystalline anatase C240

Integral voltammetric charge of the S-peaks (S1+S2; referred to the total charge) from the anodic branch of cyclic voltammograms (scan rate 0.2 mV/s) is plotted as a function of the concentration of "X-ray amorphous" (XRA) phase in the material. Dashed line is a linear fit of experimental points.

Kavan, L.; Kalbac, M.; Zukalova, M.; Exnar, I.; Lorenzen, V.; Nesper, R.; Graetzel, M.; *Chem. Mater* 2004; *16*(3); 477-485

Possible Cathodes

1. Present electro-active cathode materials :

Li_xCoO_2	550 Wh/kg at C/3
$Li_xMn_2O_4$	450 Wh/kg at 1C

Cathodes are too slow and/or too instable

1. New electro-active cathode materials :

$Li_xMn_{0.31}Co_{0.16}Ni_{0.50}Al_{0.05}O_2$	640 Wh/kg at C/4 [1,2]
Li_xFePO_4	550 Wh/kg at >1C
$Li_xV_3O_8$	800 Wh/kg at >1C

[1] Spahr, Novak, Schnyder, Haas, Nesper, *J. Electrochem. Soc.* **1998**, *145,* 1113-1121
[2] Electrode material for positive electrodes of rechargeable lithium batteries, WO0141206 **2002**

Specific Energy of VO_x Nano-Fibers

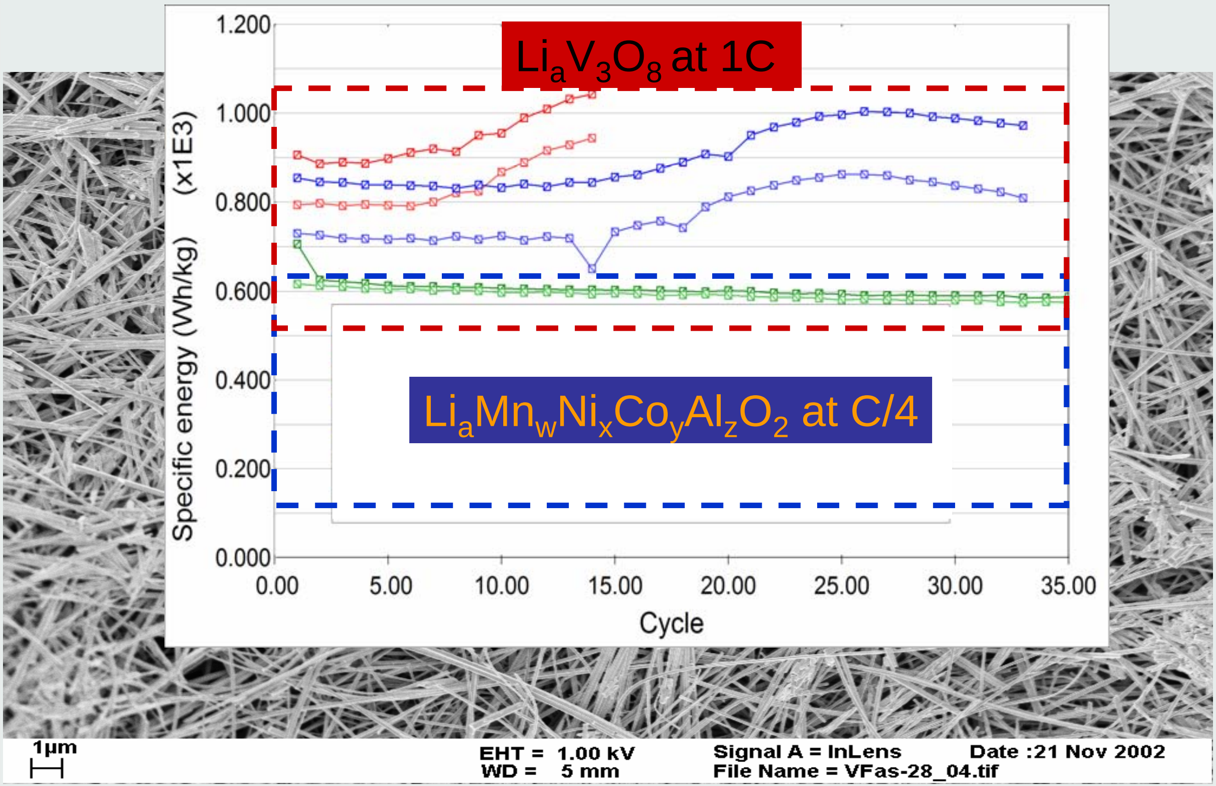

Galvanostatic Investigations of Samples with different morphologies taken at C/2, between 1.5-4.3 V.

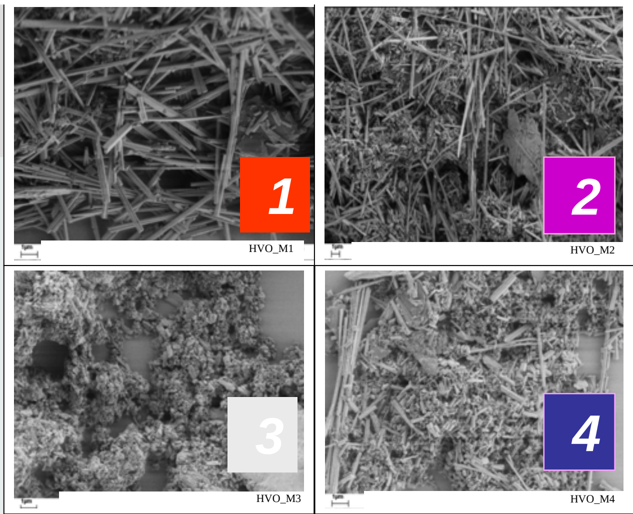

Losses by electric decoupling from base electrode

➔ Requires new electrode binding concepts

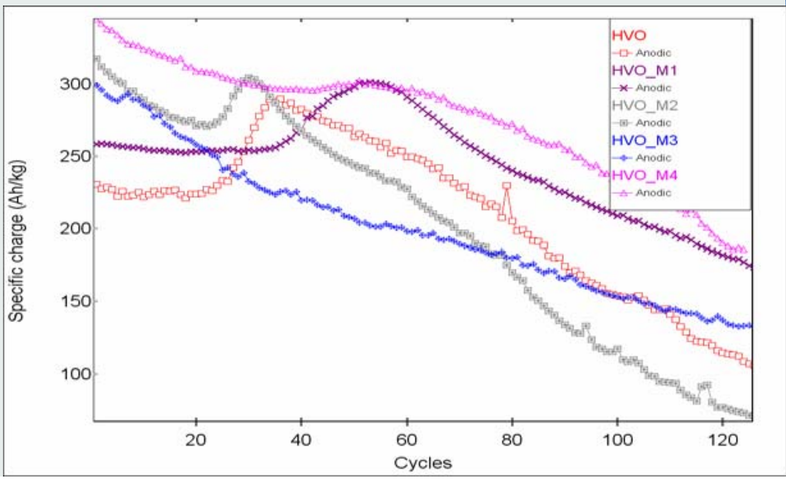

Li_xFePO_4 Nanoparticles

$LiFePO_4$ particles

New binding concept

New Fe compound at 225 Ah/kg

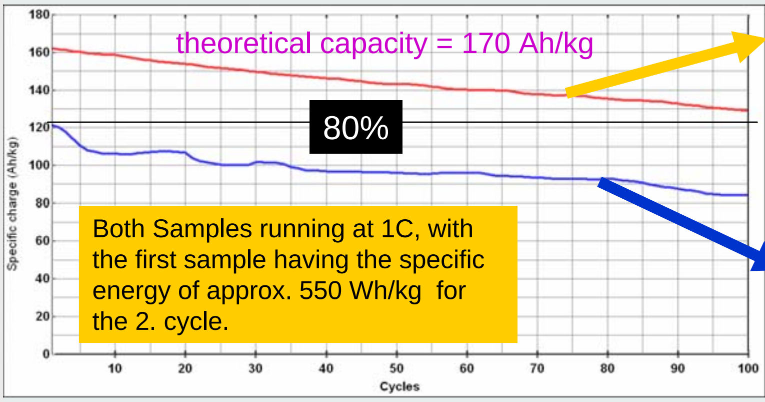

Both Samples running at 1C, with the first sample having the specific energy of approx. 550 Wh/kg for the 2. cycle.

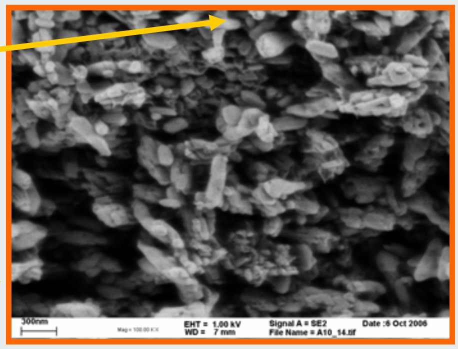

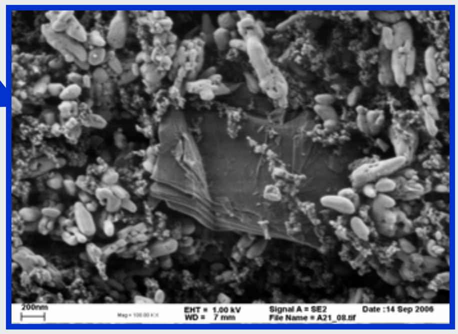

$LiFePO_4$ nanoparticles and macrosized graphite as a conductive additive (including the inert binder)

Criteria for Advanced Battery Technologies

Table I: U.S. Advanced Battery Consortium (USABC) Primary Criteria for Advanced Battery Technologies.

Power density (W/l)	600
Specific power, discharge (W/kg, 80% DOD[a]/30 s)	400
Specific power, regeneration (W/kg, 20% DOD/10 s)	200
Energy density (Wh/l, C/3[b] discharge rate)	300
Specific energy (Wh/kg, C/3 discharge rate)	200
Life (years)	10
Cycle life (cycles, 80% DOD)	1000
Power and capacity degradation (% of rated spec.)	20%
Ultimate price ($/kWh, 10,000 units @ 40 kWh)	<$100
Operating environment	−40 to 85°C
Normal recharge time	3–6 h
Fast recharge time	40–80% SOC[c] in <15 min
Continuous discharge in 1 h (no failure)	75% (of rated energy capacity)
Efficiency (C/3 discharge; 6-h charge)	80%
Self-discharge	<15% per month
Maintenance	No maintenance (service by qualified personnel only)
Abuse resistance	Tolerant (minimized by on-board controls)
Other criteria	Recyclability, 100% Packaging constraints Environmental compliance (manufacturing process, transport, in use, and recycling) Reliability (tie to warranty and cycle life) Safety constraints Vibration tolerance

Note: From Reference 54.
[a] DOD is depth of discharge.
[b] A discharge rate of C/3 means that the time for total discharge of the battery at constant current is 3 h.
[c] SOC is state of charge.

Searching New Materials for Energy Conversion and Energy Storage

R. NESPER ETH ZÜRICH & COLLEGIUM HELVETICUM

1. Renewable Energy
2. Solar Cells
3. Thermoelectricity
4. Fast High Energy Li-Ion Batteries
5. **Light Emitting Devices**
6. Hydrogen Storage
7. Luminescent Materials
8. New Materials

Light Emitting Devices - LEDs

The Semiconductor *p–n* Junction "Ultimate Lamp"

Nick Holonyak Jr.

The *p–n* junction is in fact an "ultimate lamp,"[3] by which I mean a lamp that cannot be exceeded in efficiency of converting electrical energy to optical energy. Also, as

Automobile Brake Lamps

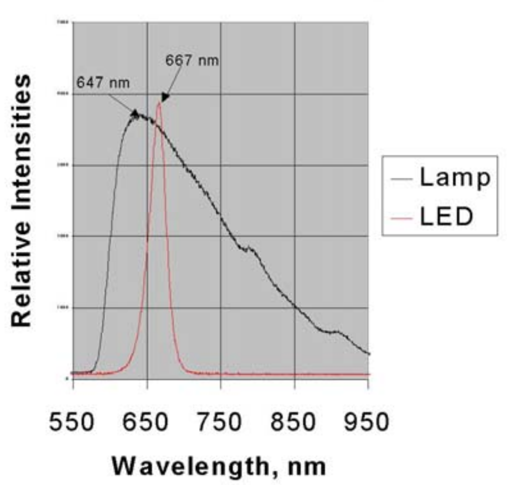

LEDs - Principles

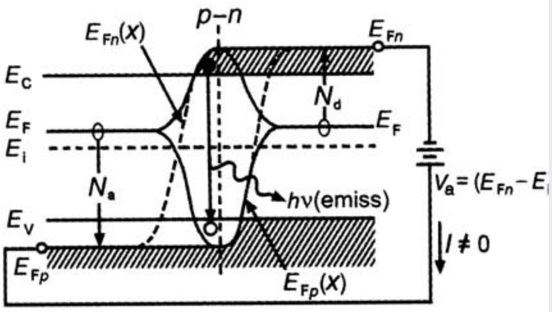

Figure 5. Photoexcitation switched off and V_a biasing the p–n junction with forward current ($I \neq 0$), thus preserving the original flat-band configuration and yielding recombination radiation $h\nu_{emiss}$. E_{Fn} and E_{Fp} are functions of the spatial variable x due to doping and voltage differences.

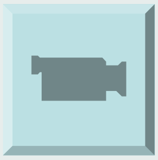

LEDs – Materials and Development

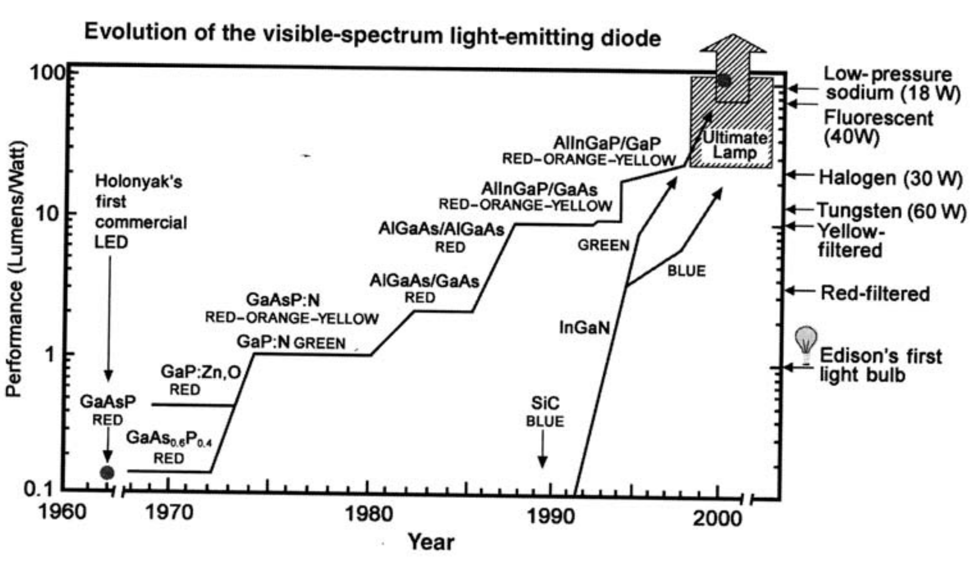

Figure 11. Diagram showing the evolution over 40 years in the performance of LEDs, from the time of the first GaAsP laser and red light-emitting diode in 1962, to the III–V alloys now prevailing in the approach to an "ultimate lamp."

LEDs – Colors and White Light

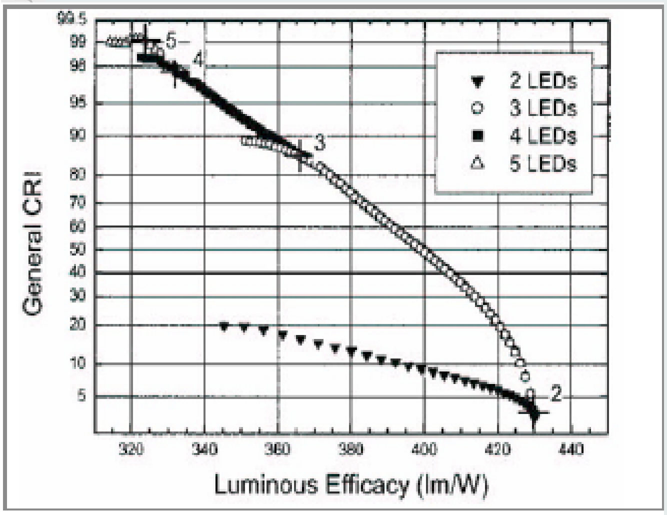

Figure 6. The envelope of maximum CRI and luminous efficacy for multi-LED white light sources with 30nm FWHM line widths and a 4870K color temperature. After A. Zukauskas, R. Vaicekauskas, F. Ivanauskas, R. Gaska, and M. S. Shur, "Optimization of white polychromatic semiconductor lamps," Applied Physics Letters 80 (2002) 234-6.

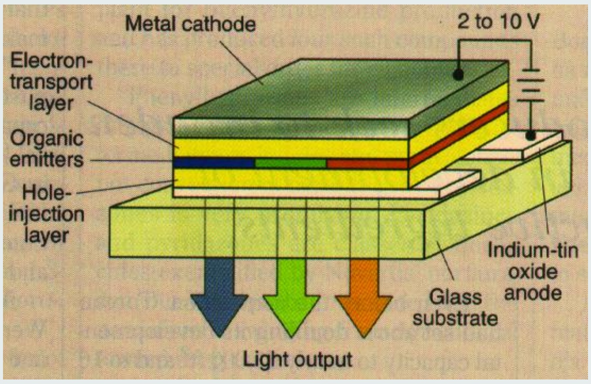

1. Generate three base colors
2. Generate UV and convert to blue, green and red

Colors and White Light

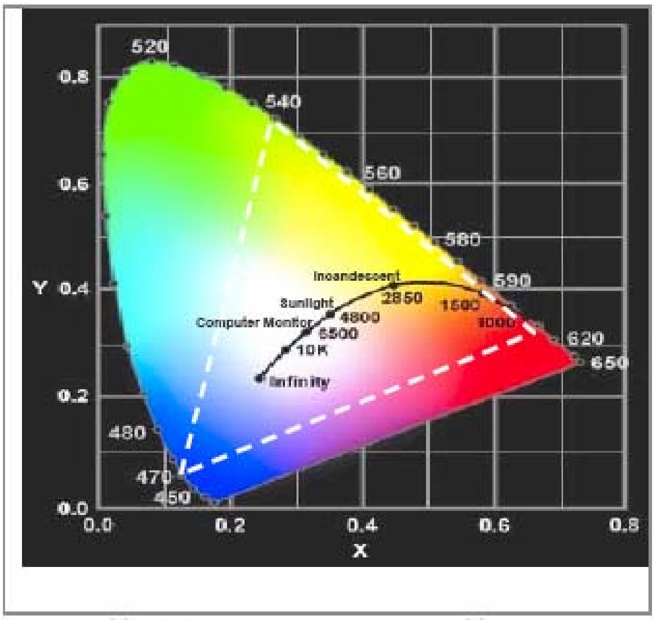

Figure 7. The CIE 1931 chromaticity diagram. The horseshoe boundary, called the spectrum locus, represents monochromatic light. The curve in the center, called the Planckian locus, represents white light. This curve traces the chromaticity coordinates of blackbodies at temperatures between 1,000 and 20,000K, which are perceived by the human visual system to be white. The vertices of the white triangle, at 460, 540 and 610nm, are the centers of the target wavelength ranges for tri-color solid-state white lighting. The interior of the triangle is the "gamut" of colors that would be available to such a light source.

Colors and White Light

R. NESPER ETH ZÜRICH & COLLEGIUM HELVETICUM

There is provided a white light illumination system including a radiation source, a first luminescent material having a peak emission wavelength of about 570 to about 620 nm, and a second luminescent material having a peak emission wavelength of about 480 to about 500 nm, which is different from the first luminescent material. The LED may be a UV LED and the luminescent materials may be a blend of two phosphors. The first phosphor may be an orange emitting Eu2+, Mn2+ doped strontium pyrophosphate, (Sr0.8Eu0.1Mn0.1)2P2O7. The second phosphor may be a blue-green emitting Eu2+ doped SAE, (Sr0.90-0.99 Eu0.01-0.1)4Al14O25. **A human observer perceives the combination of the orange and the blue-green phosphor emissions as white light.**

LEDs – Future Possibilities

HELVETICUM

Year	2002	2007	2012	2020
Luminous Efficacy (lm/W)	25	75	150	200
Lifetime (khr)	20	>20	>100	>100
Flux (lm/lamp)	25	200	1,000	1,500
Lumens Cost ($/klm)	200	20	<5	<2
Color Rendering Index (CRI)	75	80	>80	>80
Lighting Markets Penetrated	Low-flux	Incande-scent	Fluore-scent	All

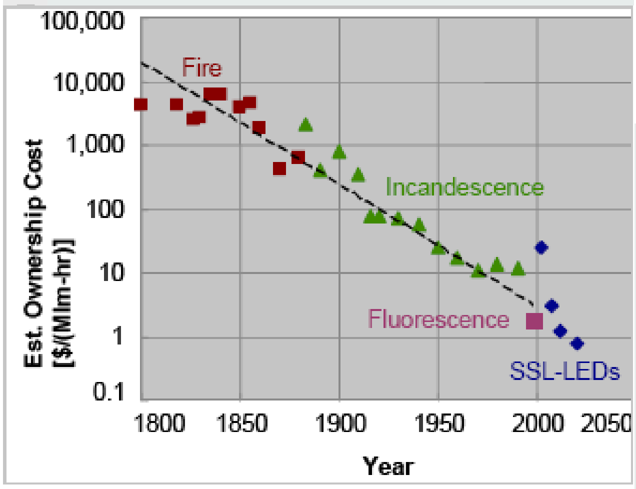

Figure 5. Estimated ownership costs of light, in 1992 dollars. Data for Fire and Incandescence for operating cost are from the work of W. Nordhaus,[6] to which estimates of capital cost have been added. Data for Fluorescence are from our estimates. Data for SSL-LEDs are the targets of this Roadmap.

LEDs – Future Possibilities

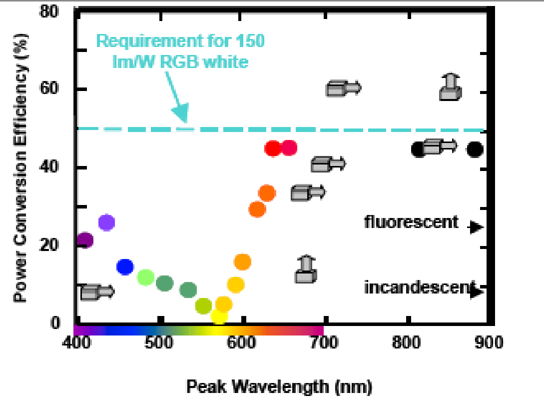

Figure 9. Power efficiency of light sources at various wavelengths. [Courtesy of M.G. Craford, LumiLeds.]

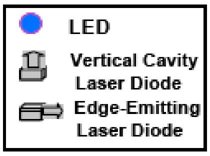

SSL-LED
targets are physically reasonable and consistent with our knowledge of fundamental physics and with other, more mature, semiconductor manufacturing technologies.

Nevertheless, solid-state lighting is in its infancy, just as silicon integrated circuits were in their infancy two decades ago.

Hence, in order to meet the lighting targets and lamp sub targets significant Challenges must be overcome in a number of areas. We organize these areas into three overall building blocks:

1. Substrates, Buffers and Epitaxy
2. Physics, Processing and Devices
3. Lamps, Luminaires and Systems

present power conversion efficiencies of infrared (710-850 nm) lasers and red (650 nm) LEDs are in the 40-60% range.

Jeff Y. Tsao, Light Emitting Diodes (LEDs) for General Illumination, AN OIDA TECHNOLOGY ROADMAP UPDATE 2 0 0 2

Future Possibilities –Nitride Phosphors

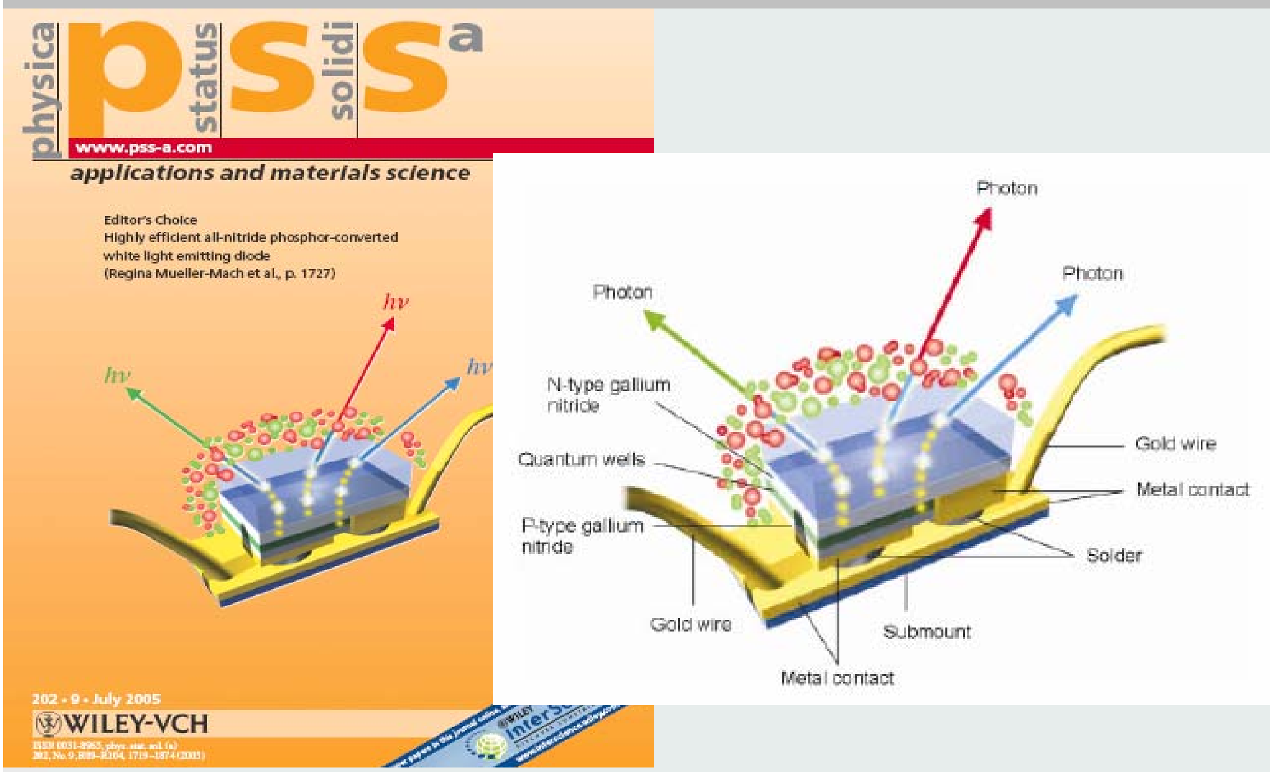

Future Possibilities –Nitride LEDs

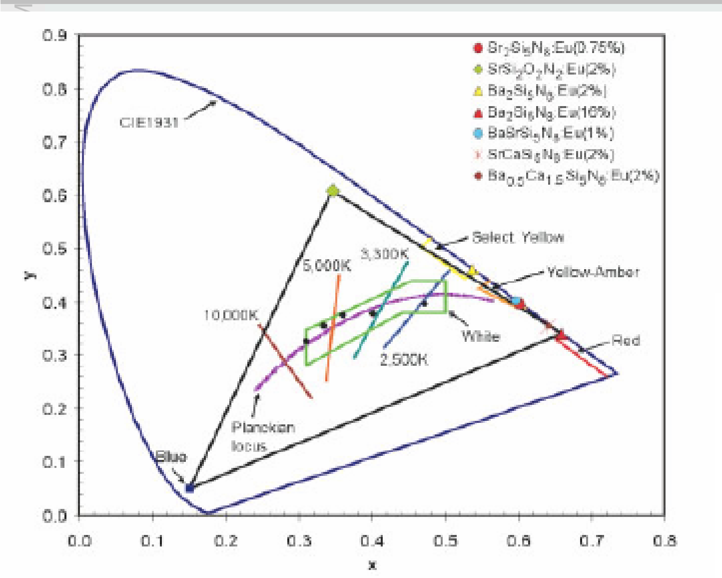

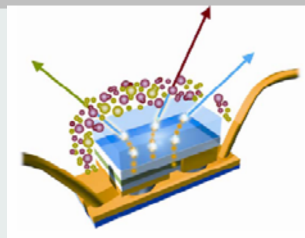

Artist's view of the 2-phosphor-converted-LED: On a copper slug and underneath a plastic lens a 'flip-chip' is soldered to metal contacts; "flip-chip" meaning the substrate on which the stack of GaN and InGaN layers has been deposited is used as light exit, the (bottom) p-contacts being highly reflective. The color converting phosphors $M_2Si_5N_8$ (orange-red) and $MSi_2O_2N_2$ (yellow-green) (M = alkaline earth) are placed on top of the chip. Primary blue as well as down-converted red and green photons are emitted.

See also:
R. Mueller-Mach, G. Mueller, M. R. Krames, H. A. Höppe, F. Stadler, W. Schnick, T. Juestel, and P. Schmidt, phys. stat. sol. (a) **202**, 1727 (2005)
http://dx.doi.org/10.1002/pssa.200520045

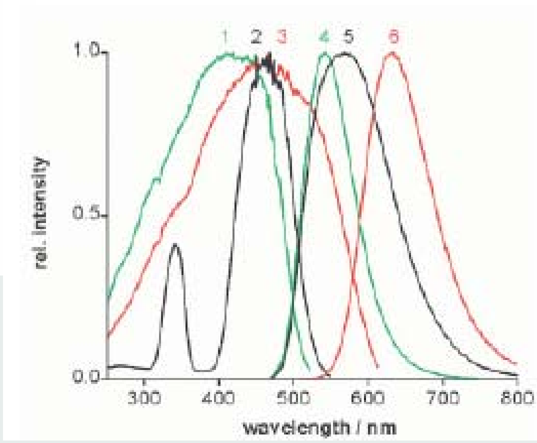

Nitride LEDs

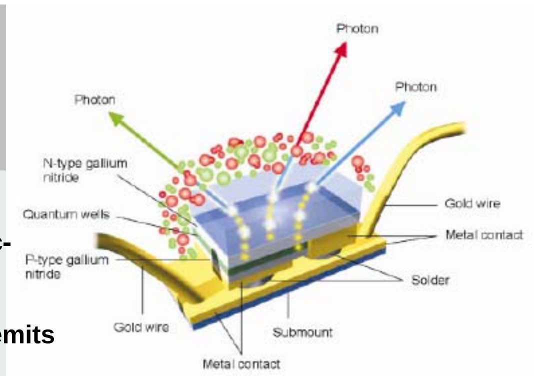

1. important new class of phosphor materials demonstrated their superior suitability for white 2-pc-LEDs.
2. alkaline earth cations of nitridosilicates and
3. oxonitridosilicates can be replaced by Eu2+, which emits for all members of these classes in the visible
4. part of the spectrum;
5. Stokes' shift is small enough to enable excitation by blue InGaN/GaN LEDs.
6. The new phosphors lend themselves to use in 2-pc-LEDs with excellent properties – a wide range of possible white light with adjustable CCT and simultaneously retained brilliant color rendering properties.
7. CCT and CRI are very stable against temperature changes and drive currents.
8. only chemically very stable materials with no environmental hazards in service, production and disposal are used.
9. Further studies to minimize photo-thermal degradation and to select the most stable stoichiometries for long-life
10. operation are underway. White LEDs may well become the next generation of general lighting sources.

Searching New Materials for Energy Conversion and Energy Storage

R. NESPER ETH ZÜRICH & COLLEGIUM HELVETICUM

1. Renewable Energy
2. Solar Cells
3. Thermoelectricity
4. Fast High Energy Li-Ion Batteries
5. Light Emitting Devices
6. **Superconducting Wires**
7. Hydrogen Storage
8. Luminescent Materials
9. New Materials

Applicable Superconductors

R. NESPER ETH ZÜRICH & COLLEGIUM HELVETICUM

1. Present HT_c Materials : Cuprates

$YBa_2Cu_3O_{7-\delta}$

Bi-based SC

...ires too expensive

...10K, undergo phase transition [1,2]

Cuprates at present not suitabel for energy transport

[1] Mourachkine, **High-Te... ...conductivity in Cuprates**, Springer 2002
[2] Bennemann, Ketter... ...es of Superconductors 1. Conventional and High-Tc-Superconductors**, Spri... ...2

2. New SC's:

MgB_2 — **T_c= 39K, good current density, H_c ~ 12Tesla on C-doping**

novel carbons ?? — **hyperbolic C's [5]**

[3] Lee et al. , Nature. 2001, 411, 558-60
[4] Fluekiger et al. , **cond-mat/0608650** 2006 & **cond-mat/0607073** 2006
[5] Nesper et al. **Hypothetical Carbon modifications with zeolith-analog structures**, *Angew.Chem. Int.Ed.Engl.* **1993**, 32, 701-703

MgB_2 - Wires

LiB → MgB_2

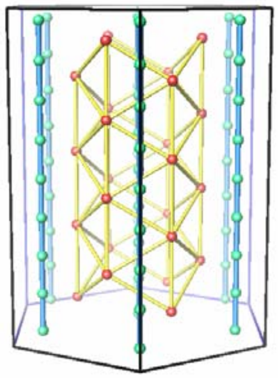

MgB_2
MgB_2C_2
LiBC
$Li_{0.5}BC$ „T_c=90K“

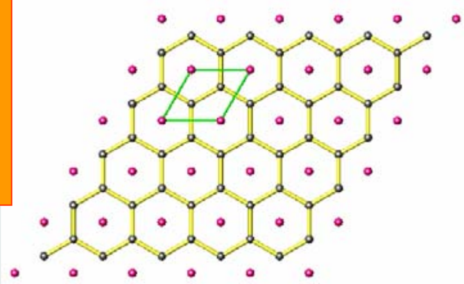

T_c= 39K, good current density, H_c ~ 12 Tesla on C-doping

Reinoso, Ottinger, Wörle, Nesper, *Method for producing a super-conducting material made of MgB_2*, Patent No WO0207149909 **2002**

Morphology Preserving Transformation

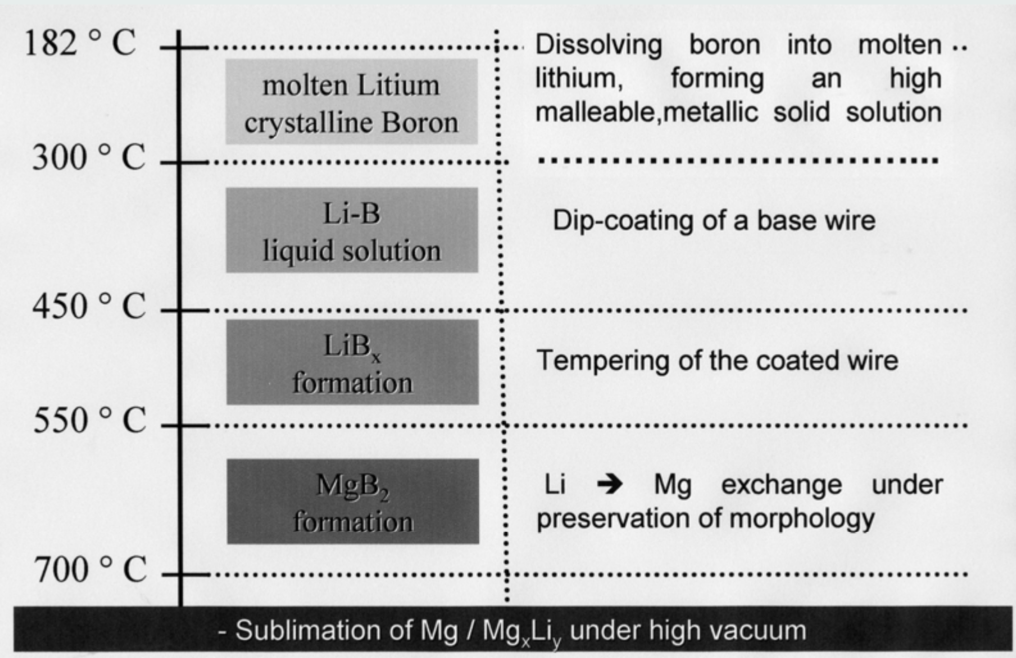

Reinoso, Ottinger, Wörle, Nesper, *Method for producing a super-conducting material made of MgB_2*, Patent No WO0207149909/2002

Searching New Materials for Energy Conversion and Energy Storage

1. Renewable Energy
2. Solar Cells
3. Thermoelectricity
4. Fast High Energy Li-Ion Batteries
5. Light Emitting Devices
6. Superconducting Wires
7. **Hydrogen Storage**
8. New Materials

Hydrogen and Energy Storage& Conversion

1. Energy:

$2H_2 + O_2 \longrightarrow 2H_2O$ -484 kJ/mol

Comparison to worst carbohydride:

$CH_4 + 2O_2 \longrightarrow CO_2 + 2H_2O$ -803kJ/mol

2. Cold combustion => no NO_x

3. No carbon burning => no CO_2 production

Hydrogen – How to Store ???

Storage	Energy Density (kWh/kg)	Rel. to Diesel (%)	(kWh/l)	Rel. to Diesel (%)	Refilling Time (min)	Notes
High pressure H_2 (300 bar)	1.00	9	0.55	7	10 to 60	Cylinder storage
Liquid H_2 (−253 °C)	6.00	55	1–1.7	12–20	up to 60	Energy loss for liquification vapo-risation loss 2%/day
Metal hydride	0.40	4	0.80	10	10	Recovery of heat 10%
Methylcyclo-hexan	0.56	5	0.37	4	10	Additional H_2 needed for dehy-dration

Ideal Electric Car

1. **Fuel cell** **=> basic power**
2. **Battery** **=> acceleration**
3. **Super-capacitors** **=> energy recoverage**
(deacceleration / breaking energy)

4. **Hydrogen as energy source**

Hydrogen pressure storage

Comparison of Hydrogen Storage Materials

S. Hynek, W.Fuller, J. Bentley, Int.J.Hydrogen Energy 22, 601 (1997)

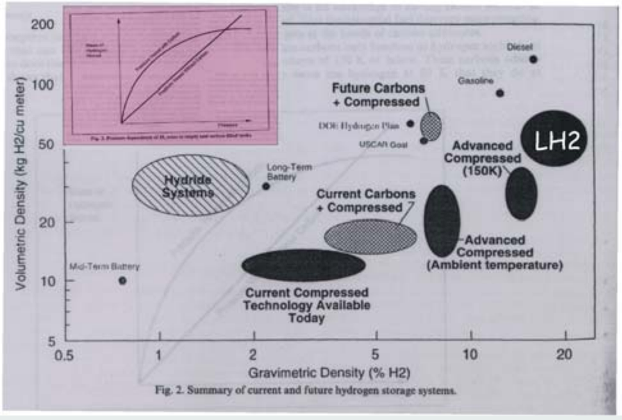

Fig. 2. Summary of current and future hydrogen storage systems.

Figure 1 Volume of 4 kg of hydrogen compacted in different ways, with size relative to the size of a car. (Image of car courtesy of Toyota press information, 33rd Tokyo Motor Show, 1999.)

Metallhydrides

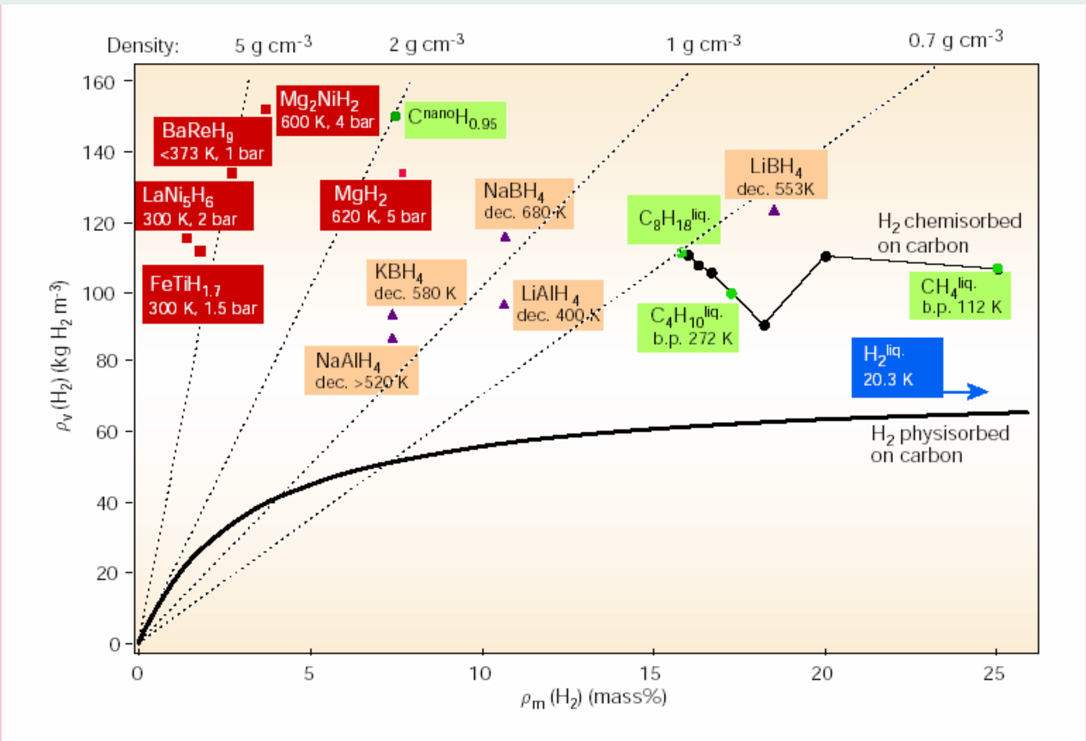

Hydrogen storage in Metal Hydrides

Table 2 Intermetallic compounds and their hydrogen-storage properties[22]

Type	Metal	Hydride	Structure	mass%	p_{eq}, T
Elemental	Pd	$PdH_{0.6}$	*Fm3m*	0.56	0.020 bar, 298 K
AB_5	$LaNi_5$	$LaNi_5H_6$	*P6/mmm*	1.37	2 bar, 298 K
AB_2	ZrV_2	$ZrV_2H_{5.5}$	*Fd3m*	3.01	10^{-8} bar, 323 K
AB	FeTi	$FeTiH_2$	*Pm3m*	1.89	5 bar, 303 K
A_2B	Mg_2Ni	Mg_2NiH_4	*P6222*	3.59	1 bar, 555 K
Body-centred cubic	TiV_2	TiV_2H_4	b.c.c.	2.6	10 bar, 313 K

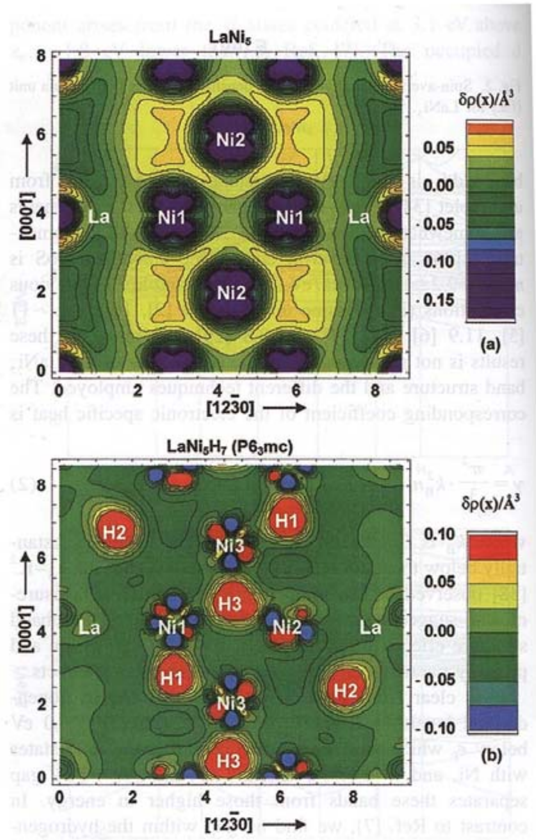

Fig. 5. Charge density differences in the $(2\bar{1}\bar{1}0)$ plane. (a) $\delta\rho = \rho(LaNi_5) - \rho(La\ atoms) - \rho(Ni\ atoms)$ for $LaNi_5$; (b) $\delta\rho = \rho(LaNi_5H_7) - \rho(LaNi_5H_0) - \rho(H\ atoms)$ for $LaNi_5H_7$.

Graphites & Heterographites ???

LiB

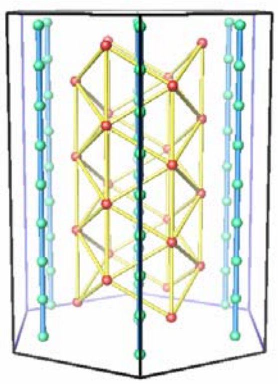

Graphites
MgB_2
MgB_2C_2
LiBC

MgB_2

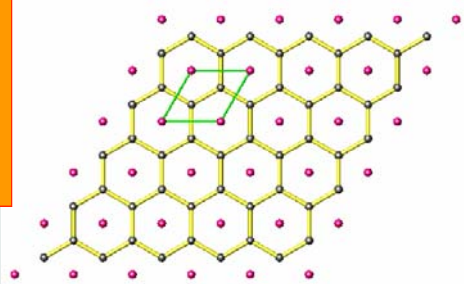

Idea :
replacing the metal–semimetal bonds by metal-H + semimetal-H bonds

„Expected advantages“:

- **Cancel the large H-element binding energies**
- **Preserve a stable structural backbone**
- **Potentially high specific H-storage up to 10 wt%**

M. J. Reinoso, Dissertation, ETH-Nr. 15781, 2004

But, Reversible H-Storage in Silicides

M. J. Reinoso, Dissertation, ETH-Nr. 15781, 2004

$Li_{12}Si_7$ – 0.5 wt%
$YbSi_{1.41}$ – 0.1 wt%

CaSi 1.6wt% ➔CaSiH
2.0 wt% ➔$CaSiH_{1.33}$ Ohba et. al.; R&D Review of Toyota 39, 40 (2004)
SrSi 1.4wt%
BaSi >2 wt%

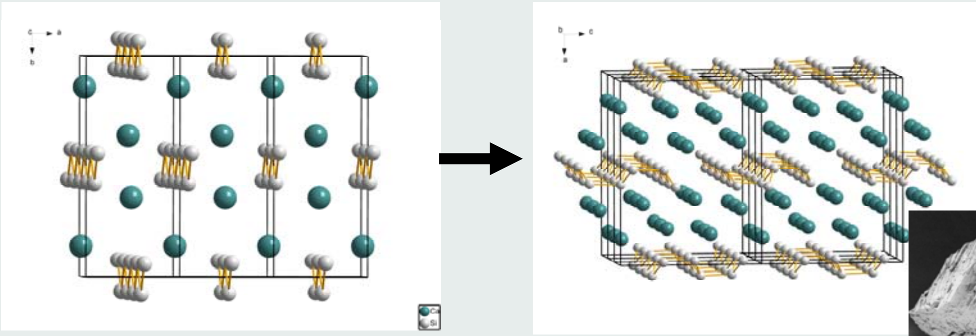

Searching New Materials for Energy Conversion and Energy Storage

1. Renewable Energy
2. Solar Cells
3. Thermoelectricity
4. Fast High Energy Li-Ion Batteries
5. Light Emitting Devices
6. Superconducting Wires
7. Hydrogen Storage
8. **New Materials**

High Temperature Polymer Si/B/C/N

M. Jansen, T. Jaeschke, B. Jaeschke, in *High Performance Non-oxide Ceramics I, Vol. 101* (Ed.: M. Jansen), Springer-Verlag, Berlin, Heidelberg, 2002, pp. 137.

Haberecht, Krumeich, Nesper, *Chem. Mater*. 16, 3, 418-423, 2004

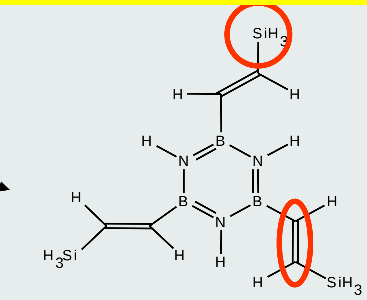

B-tris(E-silylvinyl)borazine

thermal decomp.: only H

→ 94% ceramics yield

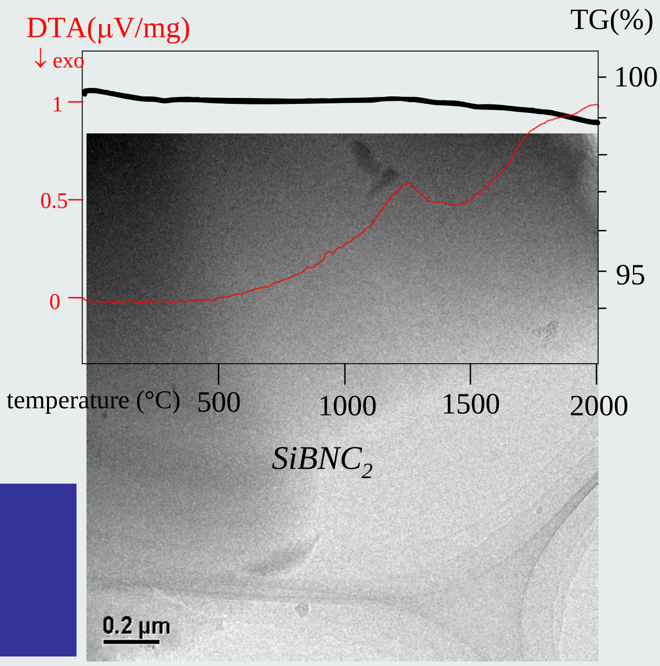

Advantages:
- High chemical & thermal stability
- Isotropic amorphous material
- Electric conductivity

Lotus effect

⇒ **BASF – Lotus Spray**

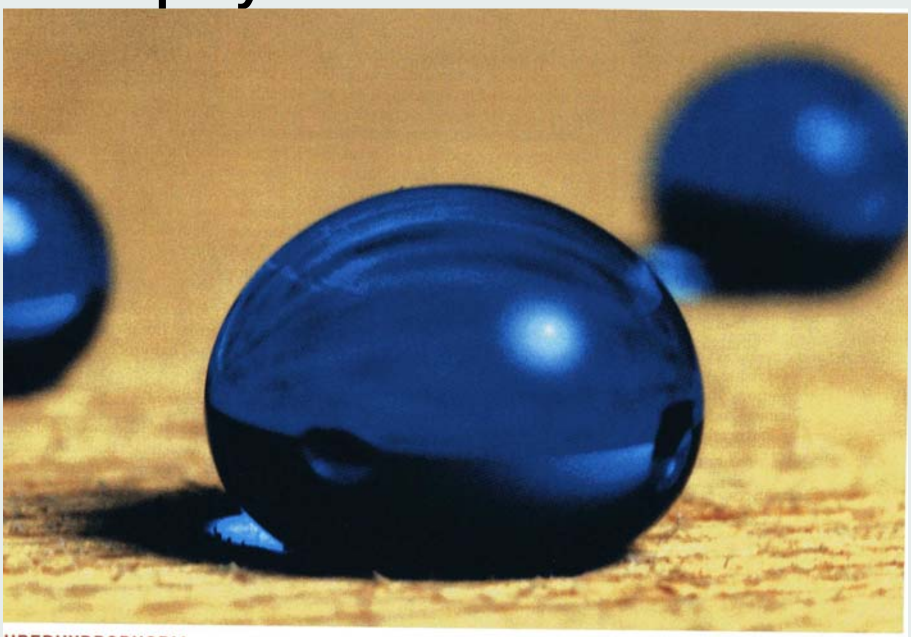

UPERHYDROPHOBIA BASF's "Lotus Spray"—using principles involving surface contact and adhesion discovered in e leaves of the lotus plant, as well as a combination of nanoparticles and very hydrophobic polymers—makes a wood rface such as that shown here extremely water-repellent and self-cleaning.

Lotus Effect by CNTs

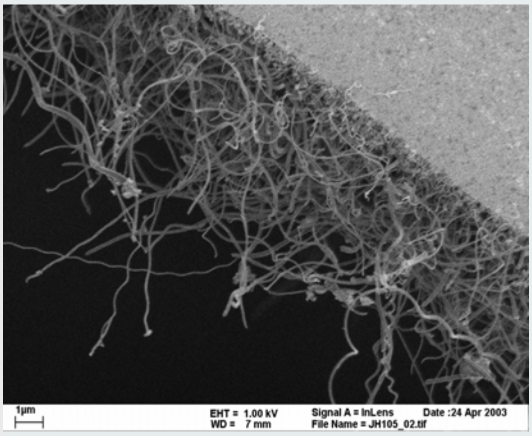

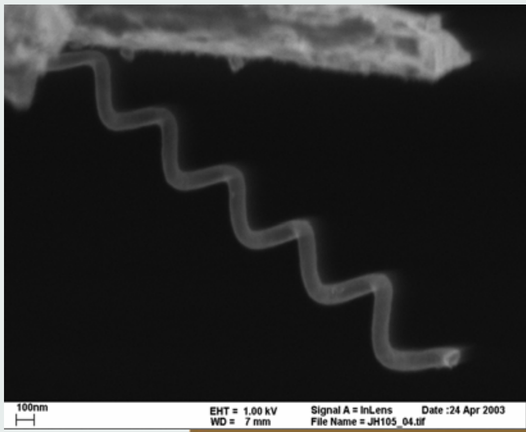

⇒ **formation of spiral-like carbon nanotubes catalyzed by Ni nano drops**

⇒ homogeneous distribution of Ni in the ceramic material: Si/Ni ratio 5.7 (= 7.5% Ni)

Lotus effect

(A) Nitrides and Nitrido Compounds

Cage compounds & Optoelektronics

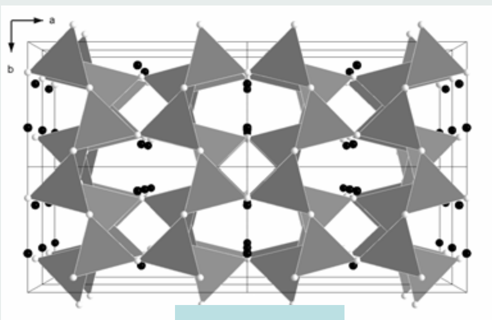

$CaSiAlN_3$

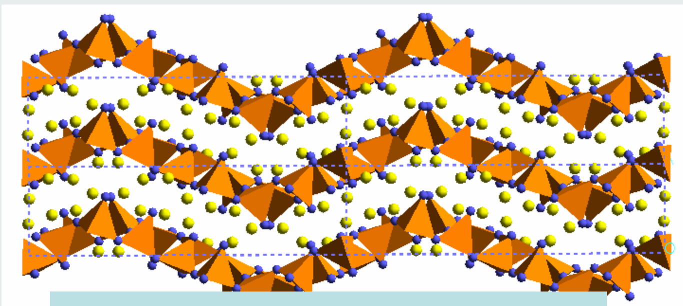

$Ca_7Si_{4-x}Al_xN_{10-x}O_x$ $(0 \leq x \leq 0.5)$

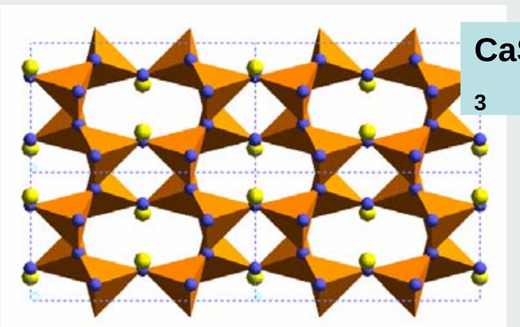

$CaSi_2N_3$

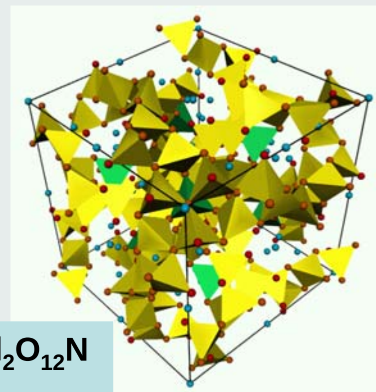

$Ca_{15}Si_{18}Al_2O_{12}N_{28}$

F. Ottinger, Dissertation, ETH-Nr. 15624, Zürich 2004

Ottinger, Nesper, Z Anorg Allg Chem 2005, 9, 631, 1597-16

Rare Earth Nitridosilicates - $Ca_{7+x}Ce_{7-x}Si_{14}N_{26}O$

New phosphors for white LEDs
Mueller-Mach, Mueller, Krames, Höppe, Stadler, Schnick, Juestel, Schmidt
phys. stat. sol. (a) 202, No. 9, 1727–1732 (2005)

$_3$ + Si; 1400 ^{o}C, 40h

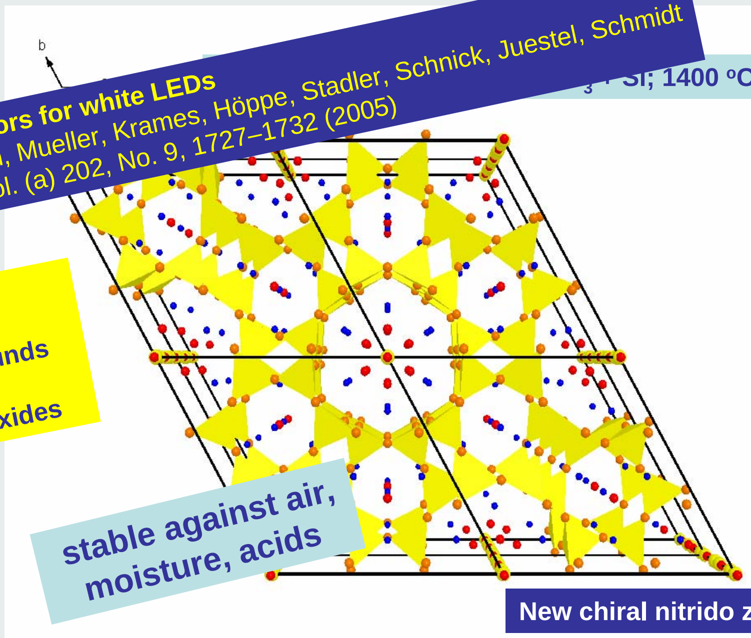

Bandgaps between 2-3 eV

Extremely stable compounds

Potentially richer than oxides

stable against air, moisture, acids

New chiral nitrido zeolite

F. Ottinger, Dissertation, ETH-Nr. 15624, Zürich 2004

Searching New Materials for Energy Conversion and Energy Storage

1. Renewable Energy
2. Solar Cells
3. Thermoelectricity
4. Fast High Energy Li-Ion Batteries
5. Light Emitting Devices
6. Superconducting Wires
7. Hydrogen Storage
8. New Materials
9. **Divers Functions**

Optical Excitations and Lasing

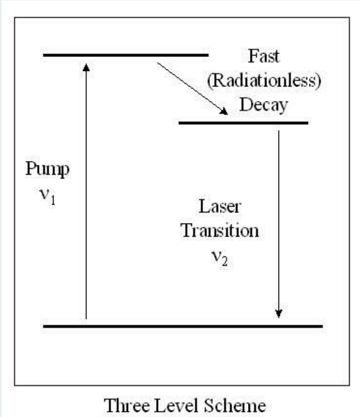

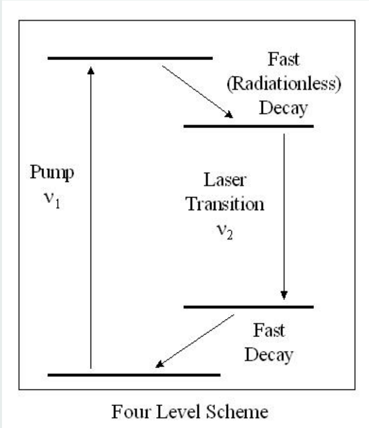

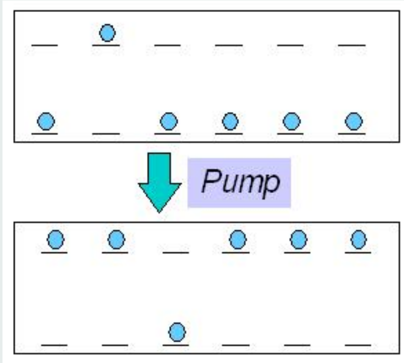

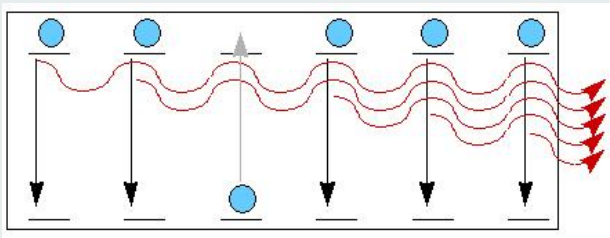

Nano-ribbon Waveguides for Subwavelength Photonics Integration

Far-field optical image of a GaN/AlGaN core–sheath-based quantum wire laser (length, 4 μm).

Lasing

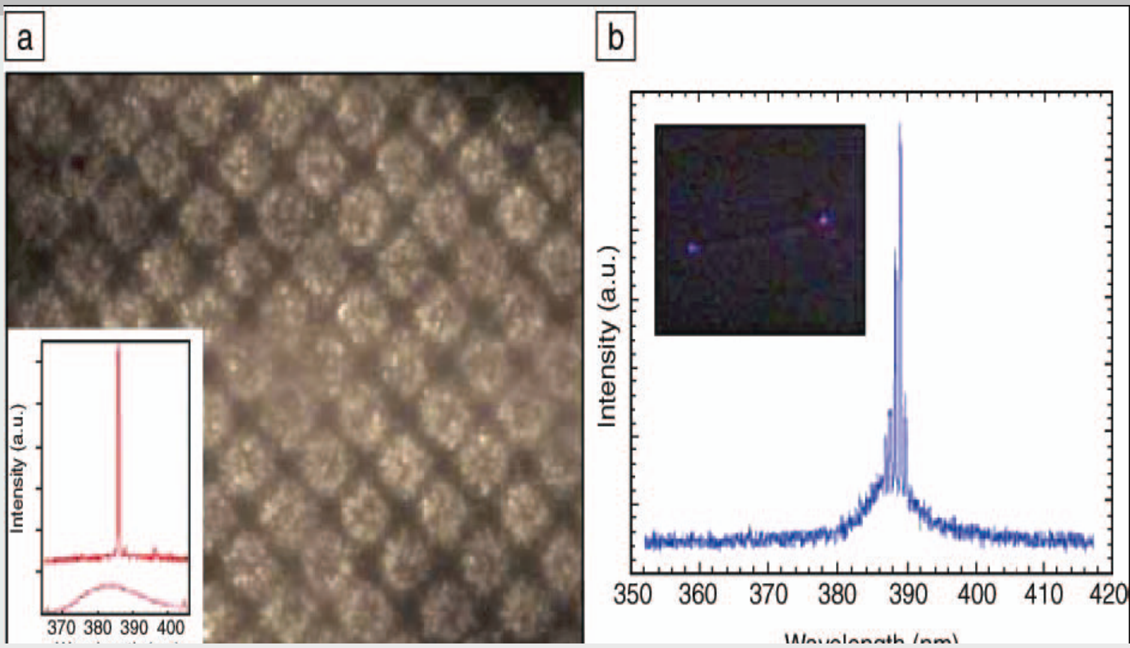

(a) Far-field optical image of patterned lasing in ZnO nanowire arrays. Each square pattern unit is 20 µm x 20 µm. Inset shows a typical emission spectrum below and above the lasing threshold. (b) Lasing spectrum from an individual ZnO nanoribbon. Inset shows a far-field optical image of the waveguiding ZnO nanoribbon (length, 35 m).

Nanoribbon Waveguides for Subwavelength Photonics Integration

Panchromatic waveguiding in a 425-m-long nanoribbon. (a) Dark-field image; cross-sectional dimensions are 520 nm 275 nm. (b) Photoluminescent (PL) image with the UV excitation spot centered near the middle of the nanoribbon, showing waveguided emission from both ends.
(c) Magnified dark-field PL view of the right end, with the laser focused on the left end. A wide (1 m) ribbon lies across the ribbon of interest.

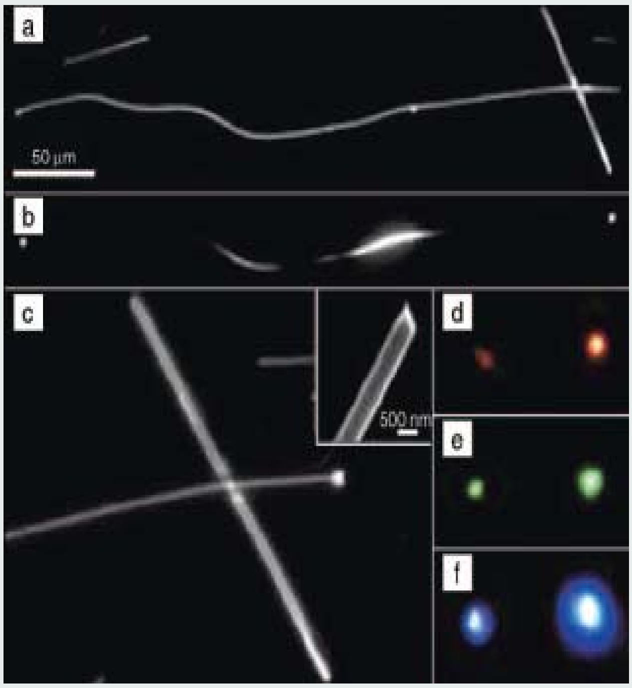

Magnet Colloids – Ferro Fluids

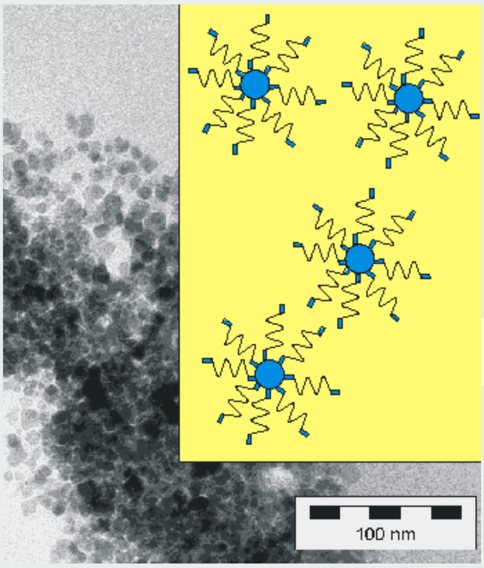

Tumor + Gene Therapy

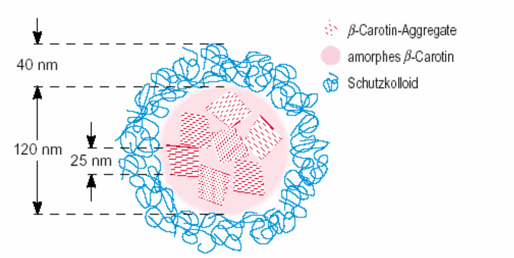

Abbildung 27. Kern-Schale-Aufbau der β-Carotin-Hydrosol-Partikel. Den spektroskopischen Daten und den Weitwinkelröntgenspektren (WAXS) zufolge besteht der Wirkstoff-Kern aus H- und J-Aggregaten mit Abmessungen bis zu 30 nm, entsprechend einer maximalen Aggregationszahl von 10000 Molekülen.

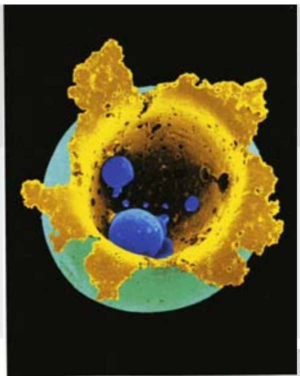

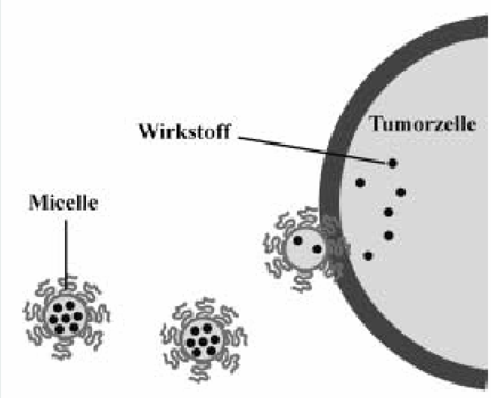

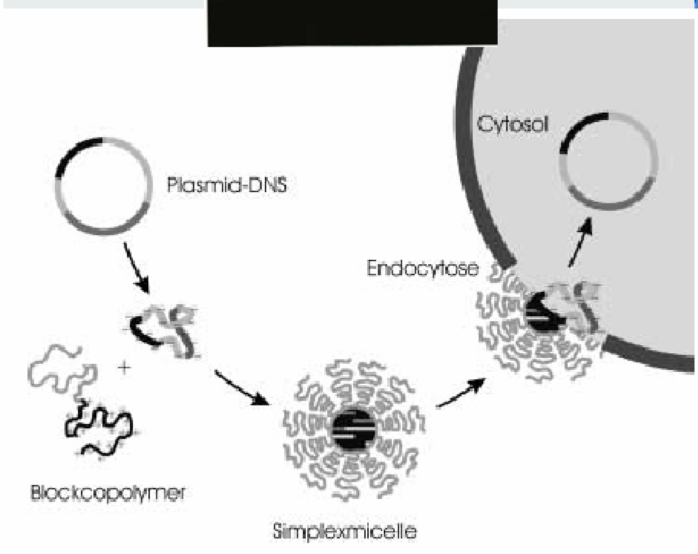

Gas Sensing

Detection of CO and O_2 Using Tin Oxide Nanowire Sensors**

By *Andrei Kolmakov, Youxiang Zhang, Guosheng Cheng, and Martin Moskovits**

Adv. Mater. **2003**, *15*, No. 12, June 17

$$O^{2-}_{(s)} \longrightarrow 1/2\ O_{2(g)} + V_0$$

$$V_0 \longrightarrow V_0^{+} + e^-$$

$$V_0^{+} \longrightarrow V_0^{++} + e^-$$

$$O^{-}_{(s)} \longrightarrow 1/2\ O_{2(g)} + e^-$$

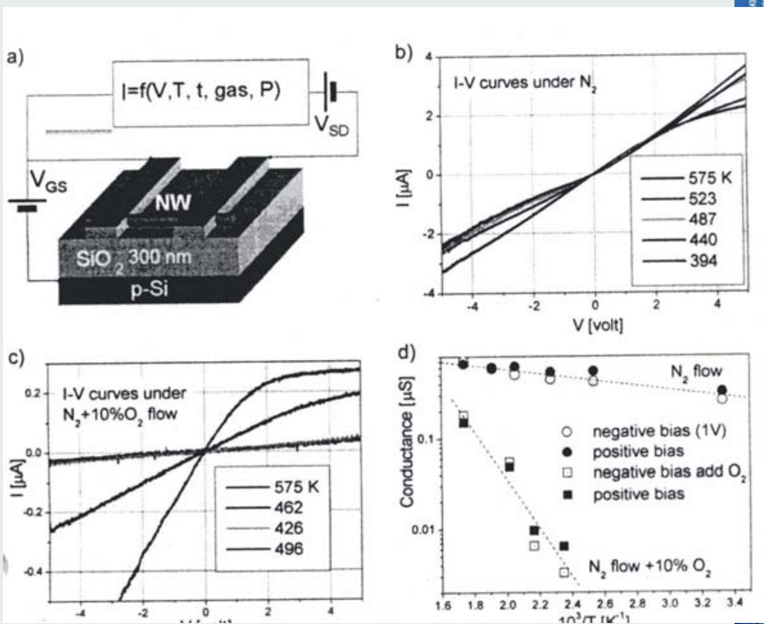

Fig. 2. Gas sensing tests on individual nanowires were carried out as a function of temperature and (flowing) ambient gas composition in a 50 mL stainless steel gas cell designed for in-situ high pressure and temperature impedance measurements. a) SnO_2 nanowires were deposited on SiO_2/Si, outfitted with vapor-deposited Au/Ti electrodes which were contacted by microscope-guided, micropositioned contacting probes. *I–V* characteristics for the nanowire measured in b) an inert, and c) an oxidizing environment. Nanowires were preconditioned for 2 h at 525 K under flowing dry N_2 before each set of measurements. The results shown were collected by first raising the nanowires to the highest temperature indicated, then decreasing the temperature incrementally and allowing thermal equilibrium to be established before the conductance was measured. d) The log of conductance versus inverse temperature for an individual SnO_2 nanowire in dry N_2 and N_2 + 10 % O_2 atmospheres. Activation energies of 46 meV and 560 meV, respectively, are determined from the slopes, the latter indicating that, in its non-conducting state, essentially all of the shallow donor states have been depleted following oxygen chemisorption.

Gas Sensing

Detection of CO and O_2 Using Tin Oxide Nanowire Sensors**

By *Andrei Kolmakov, Youxiang Zhang, Guosheng Cheng, and Martin Moskovits**

Adv. Mater. **2003**, *15*, No. 12, June 17

$$O^{2-}_{(s)} \longrightarrow 1/2\ O_{2(g)} + V_0$$

$$V_0 \longrightarrow V_0^{+} + e^-$$

$$V_0^{+} \longrightarrow V_0^{++} + e^-$$

$$O^{-}_{(s)} \longrightarrow 1/2\ O_{2(g)} + e^-$$

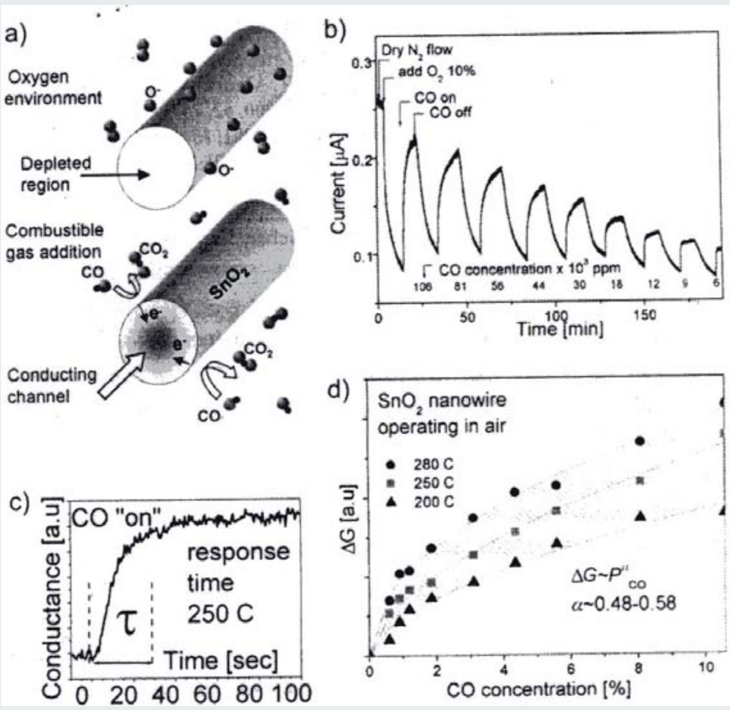

Fig. 3. The sensing mechanism of a SnO_2 nanowire involves: a) a completely depleted, hence non-conductive state under an oxidizing ambient and sharply increased conductance due to electron transfer from a surface states back into the nanowire's interior when a reducing gas (CO) is admitted. b) The response of the nanowire toward O_2 and CO pulses. The CO concentration in the flowing gas was reduced from pulse to pulse. Before the experiment was begun the nanowire was preconditioned in a constant N_2 flow. The operating voltage was 1 V, thus the ordinate corresponds to conductance in µS. c) The conductance response time of the nanowire towards 0.6 % CO pulse introduced into a background N_2 + 10 % O_2 mixture. d) The change in conductance of individual SnO_2 nanowires as a function of CO concentration at three values of the temperature. The data was fit to $\Delta G \propto P^{a}_{CO}$. The solid lines represent the best fit with exponent values ranging between 0.48 and 0.58.

Present Applicational Perspectives of Nanotechnology

Current applications
- Cosmetics
- Self-cleaning windows
- Pigments
- Stained glass windows
- Sunscreen

1-5 Years
- Security application
- Luminescent probes in biological screening applications
- Bar coding
- Chemical\biological sensors
- Coloured lighting

6-10 Years
- Flat panel displays
- Solar cells
- Date storage

10– 30Years
- light emitting diodes
- Single electron devices
- quantum computing

Where to go ?

1. Design on the nano scale
2. New compounds (nitrides?)
3. Design of new composites

Go nano

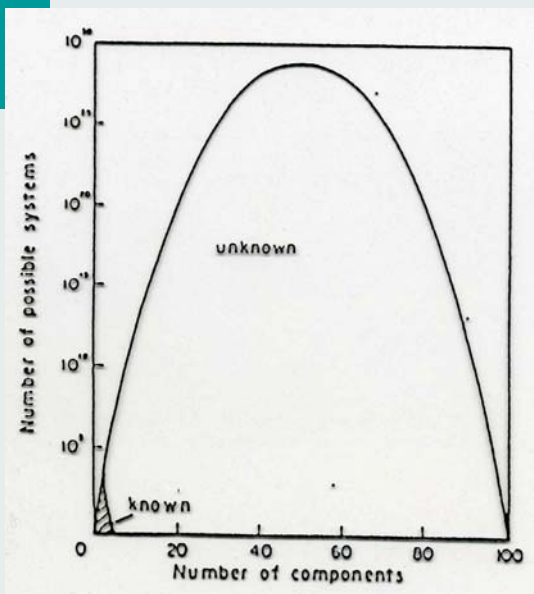

Why and when fuel cells ?

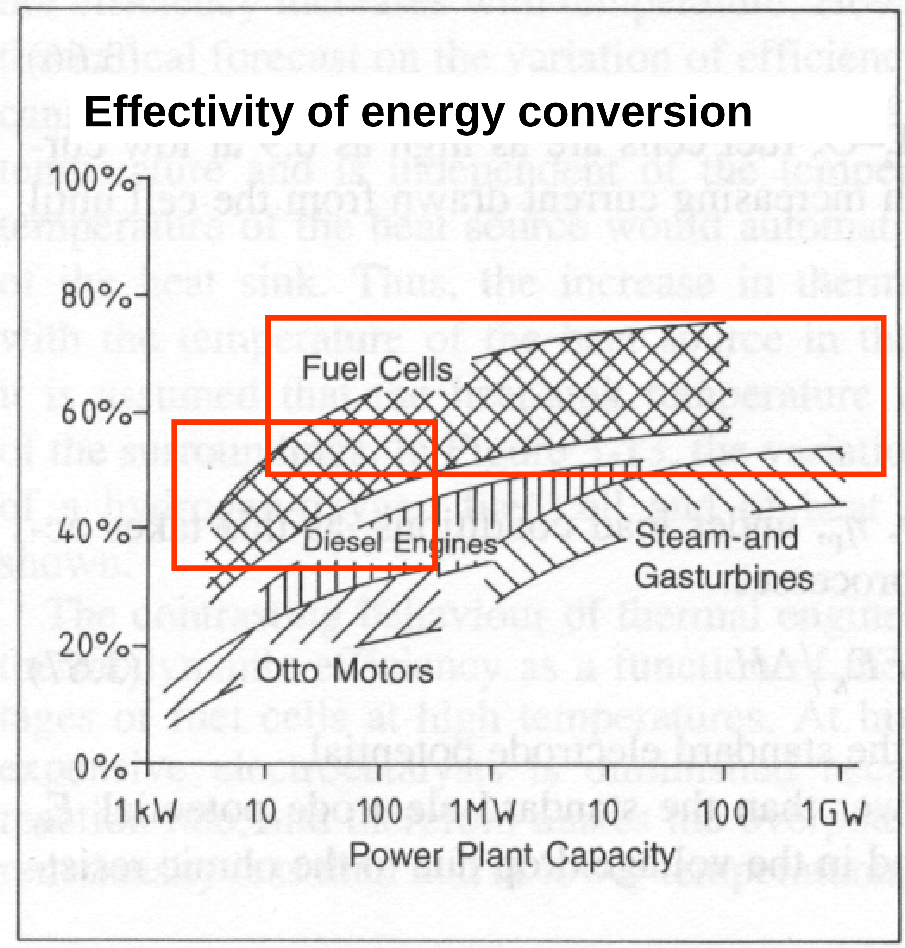

Fuel Cell- What do natural laws say?

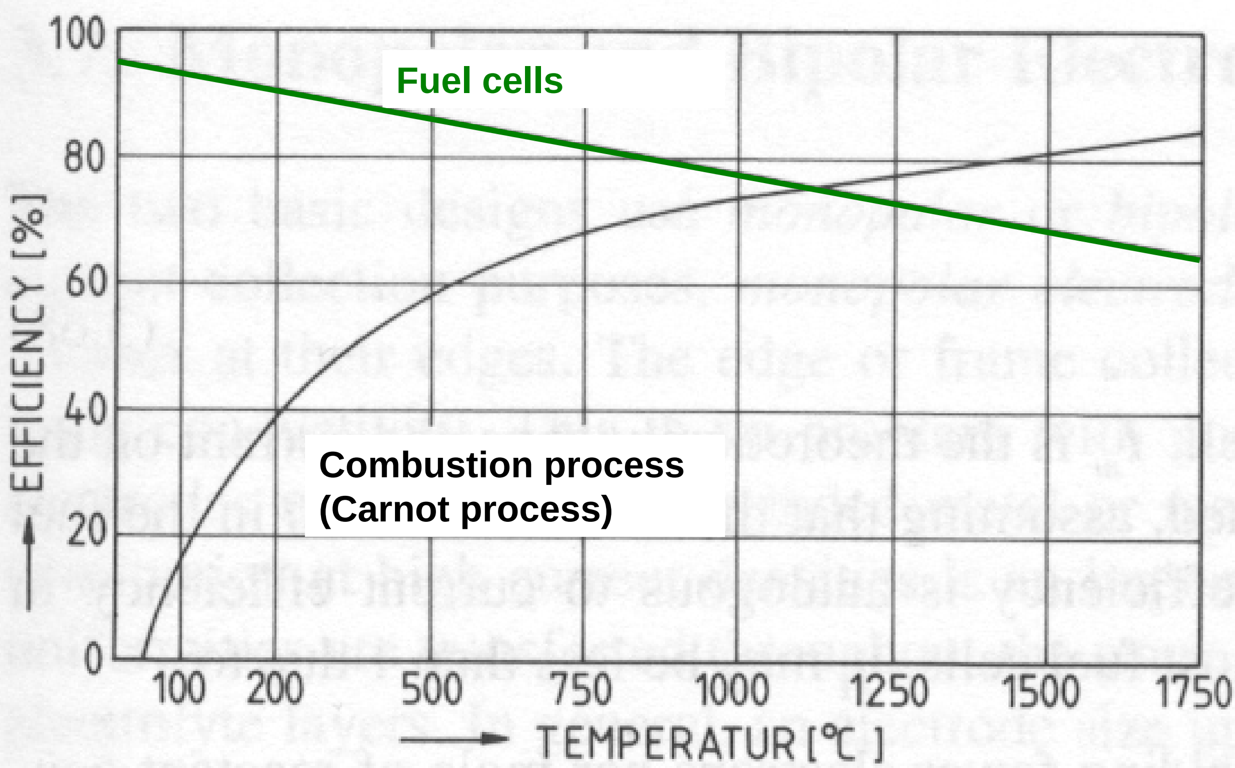

Types of fuel cells

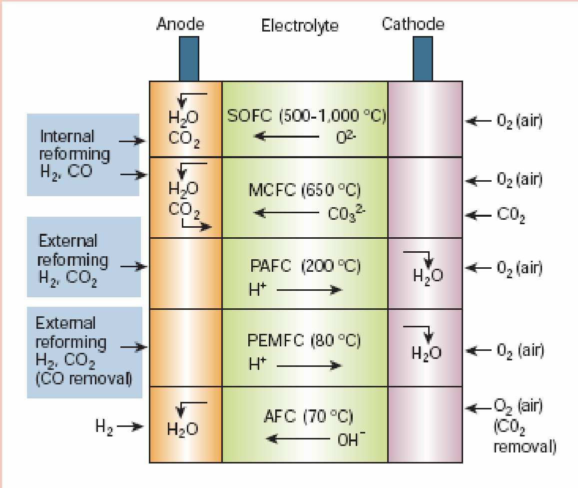

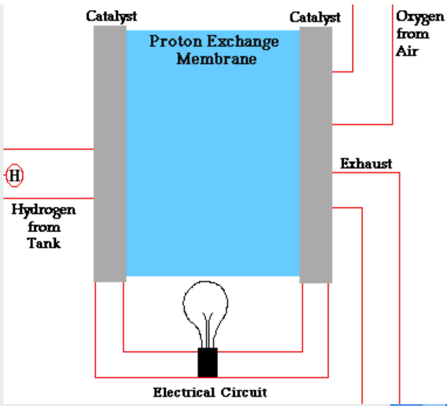

Figure 1 Summary of fuel-cell types. The oxidation reaction takes place at the anode (+) and involves the liberation of electrons (for example, $O^{2-} + H_2 = H_2O + 2e^-$ or $H_2 = 2H^+ + 2e^-$). These electrons travel round the external circuit producing electrical energy by means of the external load, and arrive at the cathode (–) to participate in the reduction reaction (for example, $1/2O_2 + 2e^- = O^{2-}$ or $1/2O_2 + 2H^+ + 2e^- = H_2O$). It should be noted that as well as producing electrical energy and the reaction products (for example, H_2O and CO_2), the fuel-cell reactions also produce heat. The reaction products are formed at the anode for SOFC, MCFC and AFC types, and at the cathode for PAFC and PEMFC types. This difference has implications for the design of the entire fuel-cell system, including pumps and heat exchangers. To maintain the composition of the electrolyte component in the MCFC system, CO_2 has to be recirculated from the anode exhaust to the cathode input. Additionally, the composition of the polymeric-membrane electrolyte has to be carefully controlled during operation by an appropriate 'water management' technology.

PEMFC Fuel Cell

working principle

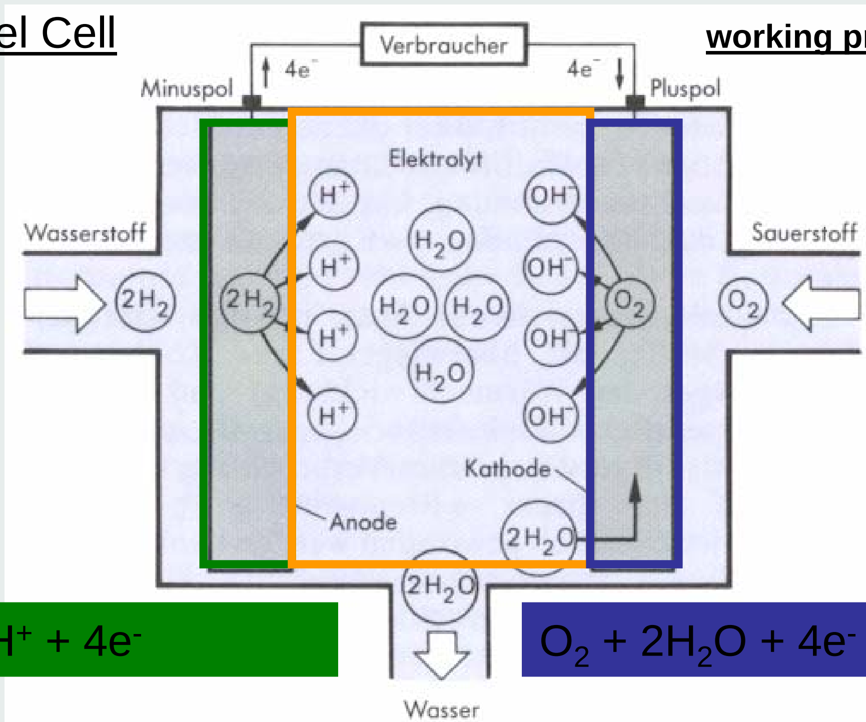

$2H_2 \Rightarrow 4H^+ + 4e^-$

$O_2 + 2H_2O + 4e^- \Rightarrow 4OH^-$

Membrane: transport of H^+ - transport of water

Fuel Cell – Working Principle

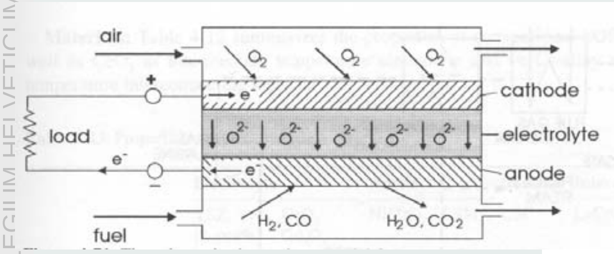

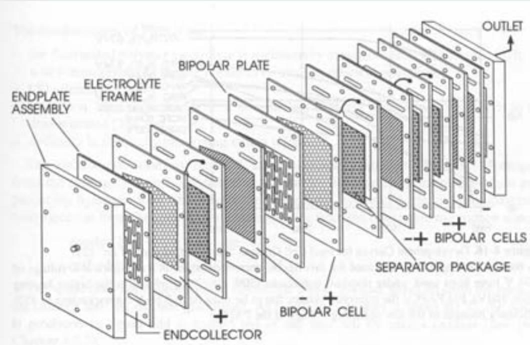

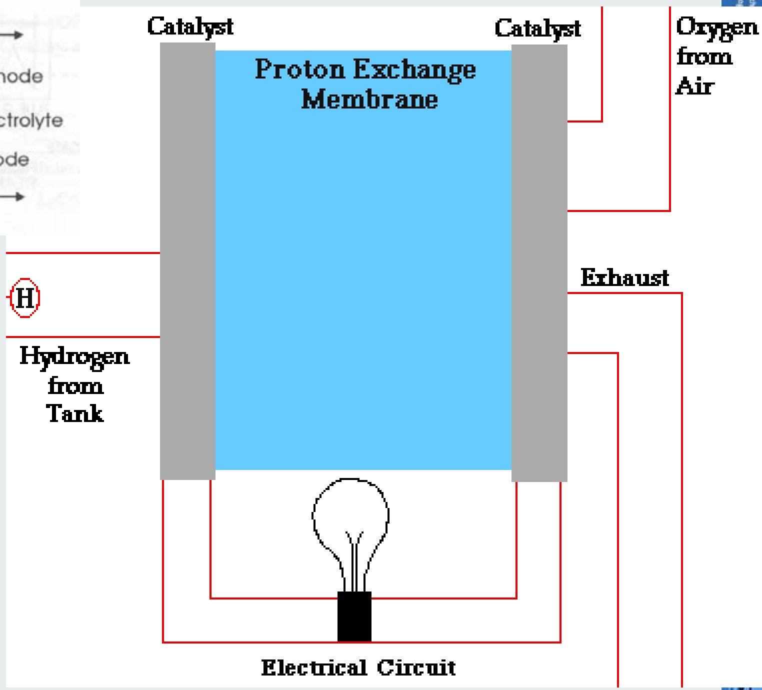

Problems – Electrolyte

select. Ion transport of H^+ or O^{2-}
channel off waste water&CO_2

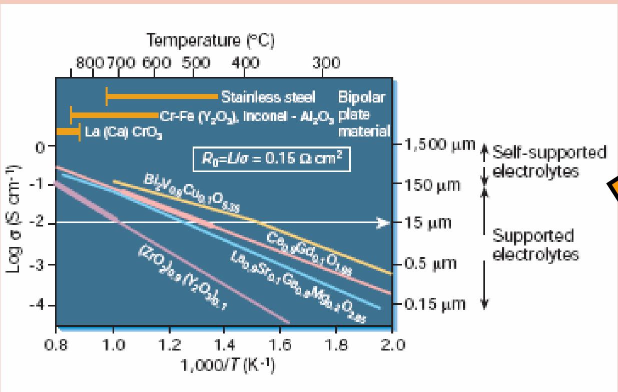

Figure 4 Specific conductivity versus reciprocal temperature for selected solid-oxide electrolytes. To ensure that the total internal resistance (that is, electrolyte + electrodes) of a fuel cell is sufficiently small, the target value for the area specific resistivity (ASR) of the electrolyte is set at 0.15 Ω cm². Films of oxide electrolytes can be reliably produced using cheap, conventional ceramic fabrication routes at thicknesses down to ~15 µm. It follows that the specific conductivity of the electrolyte must exceed 10^{-2} S cm^{-1}. This is achieved at 500 °C for the electrolyte $Ce_{0.9}Gd_{0.1}O_{1.95}$, and at 700 °C for the electrolyte $(ZrO_2)_{0.9}(Y_2O_3)_{0.1}$. Although the electrolyte $Bi_2V_{0.9}Cu_{0.1}O_{5.35}$ exhibits higher conductivities, it is not stable in the reducing environment imposed by the fuel in the anode compartment of a fuel cell.

Advantages&Disadvantages of Cell Types

Materials for fuel-cell technologies
Brian C. H. Steele, **Angelika Heinzel**
NATURE | VOL 414 | 15 NOVEMBER 2001

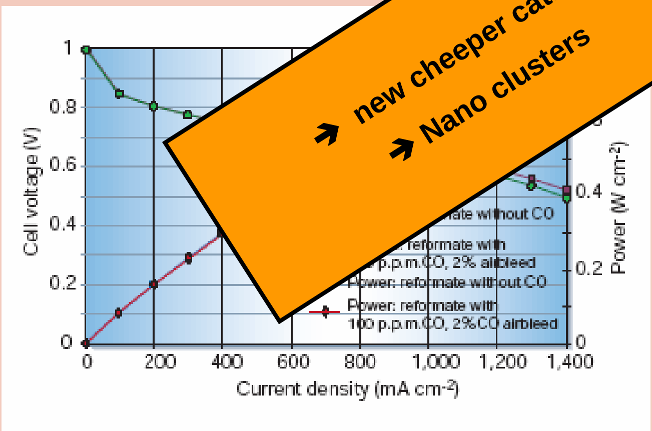

➔ new cheeper catalyst
➔ Nano clusters

Figure 3 CO tolerance on Pt/Ru anode electrodes. Active cell area, 50 cm^2; precious metal loadings, <0.4 mg cm^{-2}; temperature, 80 °C; pressure, 3 bar; anode fuel reformate, 60% H_2, 25% CO_2, 15% N_2; cathode, air. (From ref. 56.)

...mmary of future R&D requirements for fuel-cell materials

	Size (kW)	Fuel cell	Fuel	Critical materials issues
...tems ...rtable ...ectronic devices	0.001–0.05	PEMFC DMFC	H_2 CH_3OH	Membranes exhibiting less permeability to CH_3OH, H_2O
		SOFC	CH_3OH	Novel PEN structures
Micro-CHP	1–10	PEMFC	CH_4 LPG	CO-tolerant anodes, novel membranes, bipolar plates
		SOFC	CH_4 LPG	More robust thick-film PENs operating at 500–700 °C
APU, UPS, remote locations, scooters	1–10	SOFC	LPG Petrol	More robust thick-film PENs operating at 500–700 °C; rapid start-up
Distributed CHP	50–250	PEMFC	CH_4	CO-tolerant anodes, novel membranes, bipolar plates
		MCFC	CH_4	Better thermal cycling characteristics
		SOFC	CH_4	Cheaper fabrication processes; redox-resistant anodes
City buses	200	PEMFC	H_2	Cheaper components
Large power units	10^3–10^4	SOFC/GT	CH_4	Cheaper fabrication processes for tubular SOFC system

Abbreviations: UPS, uninterruptible power systems; LPG, liquid petroleum gas; GT, gas turbine. Other abbreviations defined in the text.

Ideal Electric Car

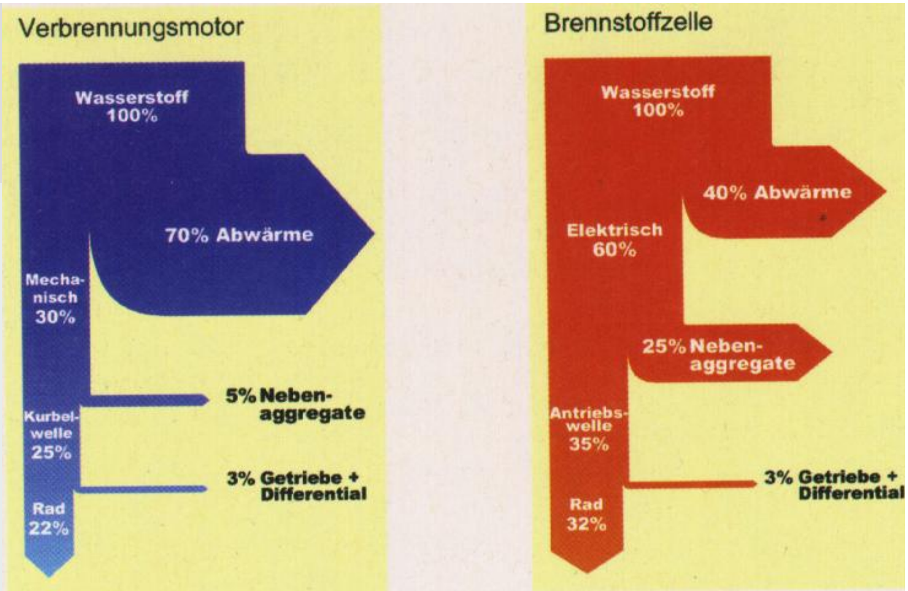

1. Fuel cell => basic energy
2. Battery => acceleration
3. Super capacitor => energy recuperation
4. Hydrogen as primary energy source

Electric Car

Disadvantages **=> technological Solution**

1. **Tire Sound level** **=> technological advance**
2. **fossile fuels** **=> renewable fuels**
3. **High temperatures** **=> fuel cell**
4. **CO_2 emission** **=> hydrogen**
5. **Emission of NO_x** **=> catalysis**

R. NESPER ETH ZÜRICH & COLLEGIUM HELVETICUM